Supporting Information

Tris-Triazolium salts as anion receptors and as precursors for the preparation of cylinder-like coordination cages

Fadi AL-Shnani,[1] Gregorio Guisado-Barrios[*],[2] Daniel Sainz ,[1] Eduardo Peris[*2]

[1]Department de Química Inorgànica i Orgànica, Universitat de Barcelona, Marti i Franquès 1, Barcelona, E-08028, Spain

[2]Institute of Advanced Materials (INAM). Universitat Jaume I. Av. Vicente Sos Baynat s/n. Castellón. E-12071. Spain. Email: eperis@uji.es

General methods

General methods. The 1,3,5-triethynylbenzene[1] and mesityl azide[2] were synthesized as previously reported. All manipulations were performed under nitrogen atmosphere using standard Schlenk techniques. Solvents were dried using a solvent purification system (MBraun SPS). All reagents were used as received from commercial suppliers. NMR spectra were recorded on Varian Innova 300 and 500 MHz spectrometers, using $CDCl_3$ and CD_2Cl_2 as solvents. Electrospray mass spectra (ESI-MS) were recorded on a Micromass Quatro LC instrument; nitrogen was employed as drying and nebulizing gas. Accurate mass measurements were performed by use of a Q-TOF premier mass spectrometer with electrospray source (Waters, Manchester, UK) operating at a resolution of ca. 16 000 (fwhm). Elemental analyses were carried out on a EuroEA3000 Eurovector Analyzer.

S1. Synthesis and characterization

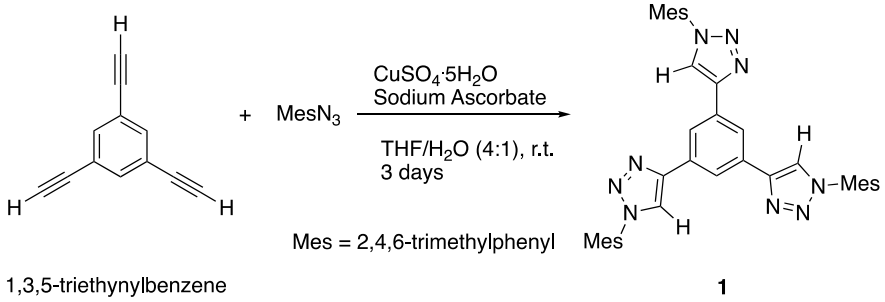

1.1 Synthesis of 1,3,5-tris(1-mesityl-1*H*-1,2,3-triazol-4-yl)benzene 1:

To a stirring solution of the 1,3,5-triethynylbenzene (0.96 g, 6.39 mmol) in tetrahydrofuran (40 mL), was added mesityl azide[2] (3.61 g, 22.31 mmol) at room temperature, followed by the addition of a mixture of copper sulfate (0.95 g, 3.83 mmol) and sodium ascorbate (7.59 g, 38.3 mmol) in water (10 mL). The solution allowed stirring for 3 days at 50° C. The reaction was quenched with a 5% aqueous solution of NH_4OH in dichloromethane. The organic layer was separated and dried with $MgSO_4$. A yellowish solid obtained after evaporation the solvent and washed with ether to have a light yellowish solid in a 74.81 % yield. ^{1}H NMR (400 MHz, $CDCl_3$): δ (ppm) 8.53 (s, 3H, C*H*$_{trz}$), 8.08 (s, 3H, C*H*$_{Ar}$), 7.03 (s, 6H, C*H*$_{Mes}$), 2.38 (s, 9H, C*H*$_3$), 2.04 (s, 18H, C*H*$_3$). ^{13}C{1H} NMR (100 MHz, $CDCl_3$): δ (ppm) δ= 147.1, 140.3, 135.2, 133.5, 132.0, 129.3, 122.9, 122.6, 21.3, 17.5. HR-MS calcd. for $[M+H]^+$: 634.3407; found $[M+H]^+$: 634.3405.

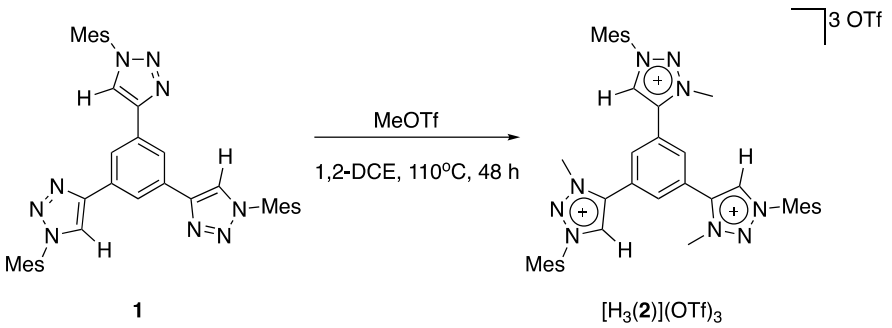

1.2 Synthesis of Synthesis of 1,3,5-Tris(1-mesityl-3-methyl-1*H*-1,2,3-triazol-3-ium)benzene Tris-(trifluoromethanesulfonate) [H3(2)](OTf)3:

In a 100 mL Schlenk flask, 1,3,5-tris(1-mesityl-1*H*-1,2,3-triazol-4-yl)benzene **1 (**0.34 g, 0.25 mmol) and methyl trifluoromethanesulfonate (0.122 g, 0.825 mmol) were combined. 1,2-dichloroethane (10 mL) was added, the heterogeneous suspension was stirred at 110° C for 48 hours. After evaporation of all volatiles and washing of the residue with diethyl ether, an off-white solid obtained in 87.04% yield. ^{1}H NMR (400 MHz, CD_3CN): δ (ppm) 9.00 (s, 3H, C*H*$_{trz}$), 8.49 (s, 3H, C*H*$_{Ar}$), 7.21 (s, 6H, C*H*$_{Mes}$), 4.50 (s, 9H, N-C*H*$_3$), 2.41 (s, 9H, C*H*$_3$), 2.18 (s, 18H, C*H*$_3$). ^{13}C{1H} NMR (100 MHz, CD_3CN): δ (ppm) δ= 143.9, 142.5, 135.8, 135.1, 132.8, 132.3, 130.8, 126.1, 40.5, 21.3, 17.4. HR-MS calcd. for $[M(OTf)_2]^+$ = 976.3073, found = 976.3079; (15V, *m/z*): 413.67 $[M]^{2+}$, 226.13 $[M]^{3+}$.

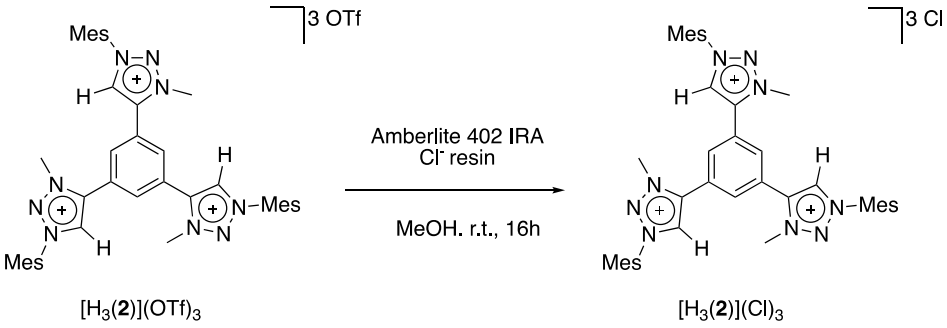

1.3 Synthesis of Synthesis of 1,3,5-Tris(1-mesityl-3-methyl-1*H*-1,2,3-triazol-3-ium)benzene trichloride [H3(2)](Cl)3:

The entitled compound was prepared by adapting a reported method in the literature.[3] To a 100 mL Schlenk containing [H3(**2**)](OTf)3 **(**0.8 g, 0.71 mmol) and Amberlite 402 IRA Cl resin (8 g) was added methanol (80 mL). The reaction mixture was stirred at room temperature for 16 hours. The resin was then removed by filtration and washed with dichloromethane (3 x 20 mL). After

evaporation, an off-white solid obtained in 98.59% yield. ^{1}H NMR (400 MHz, CD_2Cl_2): δ (ppm) 10.29 (s, 3H, C*H*$_{trz}$), 9.61 (s, 3H, C*H*$_{Ar}$), 7.11 (s, 6H, C*H*$_{Mes}$), 4.92 (s, 9H, N-C*H*$_3$), 2.40 (s, 9H, C*H*$_3$), 2.24 (s, 18H, C*H*$_3$). ^{13}C{1H} NMR (100 MHz, CD_2Cl_2): δ (ppm) δ= 143.5, 142.5, 135.6, 135.4, 134.5, 132.2, 130.6, 125.9, 41.9, 21.8, 18.4. HR-MS (15V, *m/z*): 356.68 $[M]^{2+}$, 226.13 $[M]^{3+}$.

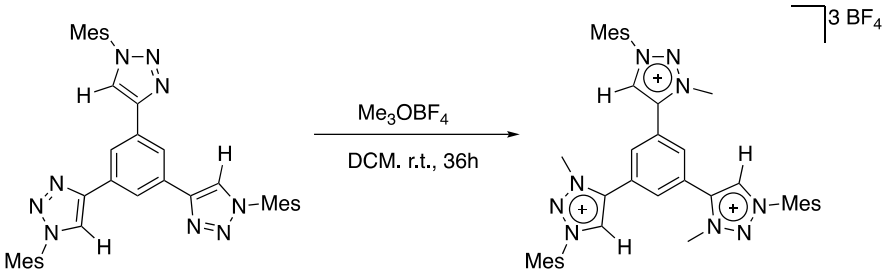

1 $[H_3(\mathbf{2})](BF4)_3$

1.4. Synthesis of 1,3,5-Tris(1-mesityl-3-methyl-1*H*-1,2,3-triazol-3-ium)benzene tris-(tetrafluoro borate) $[H_3(2)](BF_4)_3$:

In a 100 mL Schlenk flask, 1,3,5-tris(1-mesityl-1*H*-1,2,3-triazol-4-yl)benzene **1 (**0.158 g, 0.25 mmol) and Me_3OBF_4 (0.122 g, 0.825 mmol) were combined. Dichloromethane (10 mL) was added, and the heterogeneous suspension was stirred at room temperature for 36 hours. The reaction was diluted with 35 mL of $CHCl_3$ and quenched on ice by the slow addition of 10 mL of water. The organic layer was removed, then dried with $MgSO_4$. After filtration, evaporation of all volatiles an off-white solid obtained with 88% yield. ^{1}H NMR (400 MHz, CD_3CN): δ (ppm) 8.87 (s, 3H, C*H*$_{trz}$), 8.44 (s, 3H, C*H*$_{Ar}$), 7.22 (s, 6H, C*H*$_{Mes}$), 4.48 (s, 9H, N-C*H*$_3$), 2.41 (s, 9H, C*H*$_3$), 2.18 (s, 18H, C*H*$_3$). ^{13}C{1H} NMR (100 MHz, CD_3CN): δ (ppm) δ= 144.0, 142.6, 135.9, 135.1, 135.7, 132.4, 130.8, 126.1, 40.5, 21.3, 17.4. HR-MS (*m/z*): 382.7 $[M]^{2+}$, 226.13 $[M]^{3+}$.

1.5. Synthesis of $[Ag_3(2)_2](Cl)_3$

$[H_3(\mathbf{2})](Cl)_3$ (0.100 g, 0.127 mmol), Ag_2O (0.044 g, 0.191 mmol) were added to methanol (15 mL). The resulting suspension was heated to 60 °C for 48 h under exclusion of light. After cooling of the reaction mixture to ambient temperature, the obtained suspension was filtered under inert gas atmosphere through a celite to get a clear solution. The filtrate was concentrated to 1 mL and addition of 15 mL of hexane resulted in the precipitation of a white solid. The precipitate was filtered off, washed with hexane and dried in vacuo. Yield: 0.106 g (93.65%). ^{1}H NMR (400 MHz

CD_2Cl_2): δ (ppm) 7.64 (s, 3H, C*H*$_{Ar}$), 6.99 (s, 6H, C*H*$_{Mes}$), 4.39 (s, 9H, N-C*H*$_3$), 2.48 (s, 18 C*H*$_{3\ Mes}$), 1.72 (s, 35 C*H*$_{3\ Mes}$). ^{13}C{1H} NMR (100 MHz, CD_2Cl_2): δ (ppm) δ= 169.5 (dd, $^1J_{C\text{-}Ag^{107}}$ = 169.5 Hz, $^1J_{C\text{-}Ag^{109}}$ = 168.8 Hz), 147.8, 140.8, 136.5, 134.4, 133.3, 129.6, 129.5, 39.6, 21.4, 17.4. HR-MS (15V, *m/z*): 855.3 $[M]^{2+}$, 557.5 $[M]^{3+}$.

1.6. Synthesis of $[Ag_3(2)_2](BF_4)_3$

$[H_3(\mathbf{2})](BF_4)_3$ (0.100 g, 0.106 mmol) and Ag_2O (0.129 g, 0.556 mmol) were added to (15 mL) acetonitrile. The resulting suspension was heated to 55 °C for 72 h under exclusion of light. After cooling of the reaction mixture to ambient temperature, the obtained suspension was filtered under inert gas atmosphere through a celite to get a clear solution. The filtrate was concentrated to 1 mL and addition of 15 mL of hexane resulted in the precipitation of a brown solid. The precipitate was filtered off and dried under vacuo. Yield: 0.096 g (92.45%). ^{1}H NMR (400 MHz, CD_3CN): δ (ppm) 7.67 (s, 3H, C*H*$_{Ar}$), 7.05 (s, 6H, C*H*$_{Mes}$), 4.12 (s, 9H, N-C*H*$_3$), 2.47 (s, 9 C*H*$_{3\ Mes}$), 2.15 (s, 9 C*H*$_{3\ Mes}$), 1.96 (s, 9 C*H*$_{3\ Mes}$). ^{13}C{1H} NMR (100 MHz, CD_2Cl_2): δ (ppm) δ= 169.3, 147.1, 141,4, 136.6, 134.6, 132.3, 130.2, 129.8, 39.5, 21.3, 17.8. HR-MS (15V, *m/z*): 1849.6 $[M]^+$, 880.2 $[M]^{2+}$, 557.8 $[M]^{3+}$.

1.7. Synthesis of $[Au_3(2)_2](Cl)_3$

$[Ag_3(\mathbf{2})_2](Cl)_3$ (20 mg, 0.011 mmol) and $[AuCl(SMe_2)]$ (9.7 mg, 0.033 mmol) were added to (30 mL) dichloromethane and stirred at room temperature for 5 days under exclusion of light. The obtained suspension was filtered under inert gas atmosphere through a celite to get a clear solution. The filtrate was concentrated to 1 mL and addition of 15 mL of hexane resulted in the precipitation of a white solid. The precipitate was filtered off and dried under vacuo. Yield: 0.096 g (92.45%). ^{1}H NMR (400 MHz, CD_2Cl_2): δ (ppm) 7.67 (s, 6H, C*H*$_{Ar}$), 6.99 (s, 12H, C*H*$_{Mes}$), 4.40 (s, 18H, N-C*H*$_3$), 2.49 (s, 18 C*H*$_{3\ Mes}$), 2.13 (s, 18 C*H*$_{3\ Mes}$), 1.62 (s, 18 C*H*$_{3\ Mes}$).^{13}C{1H} NMR (100 MHz, $CDCl_3/CD_2Cl_2$): δ (ppm) δ= 174.6 (C-Au), 146.8, 141.1, 135.5, 134.5, 133.5, 129.7, 128.6, 40.1, 21.6, 17.5. HR-MS (15V, *m/z*): 988.3 $[M]^{2+}$, 647.2 $[M]^{3+}$.

S2. NMR Spectra

2.1. ^{1}H and ^{13}C NMR spectra of **1** in $CDCl_3$

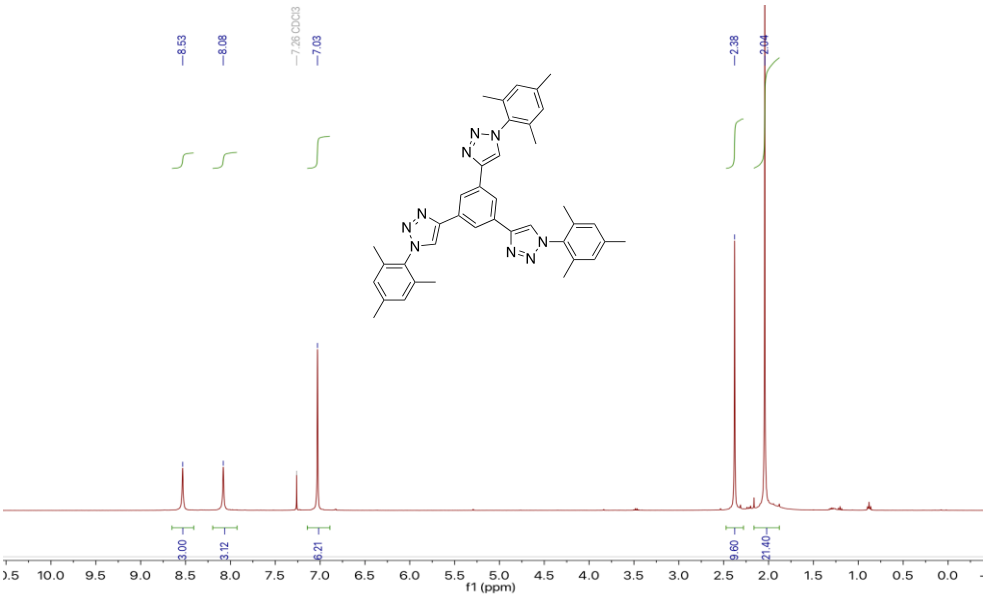

Figure S1. ^{1}H spectrum of **1** in $CDCl_3$

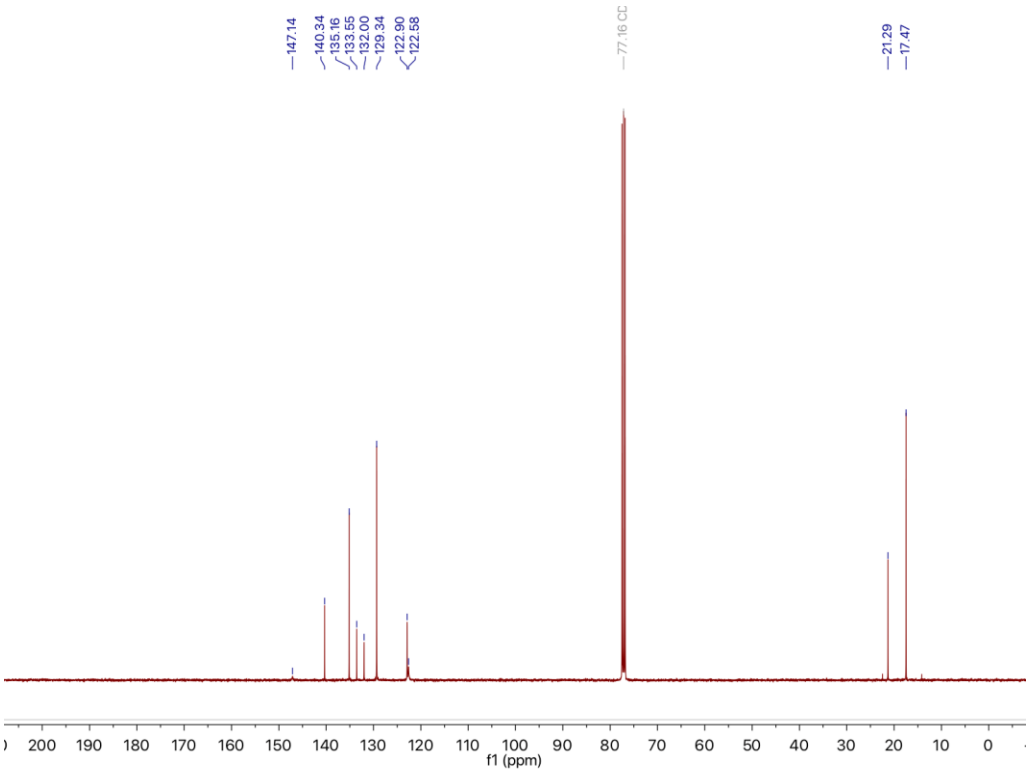

Figure S2. ^{13}C spectrum of **1** in $CDCl_3$

2.2. ^{1}H and ^{13}C NMR spectra of $[H_3(\mathbf{2})](OTf)_3$ in CD_3CN

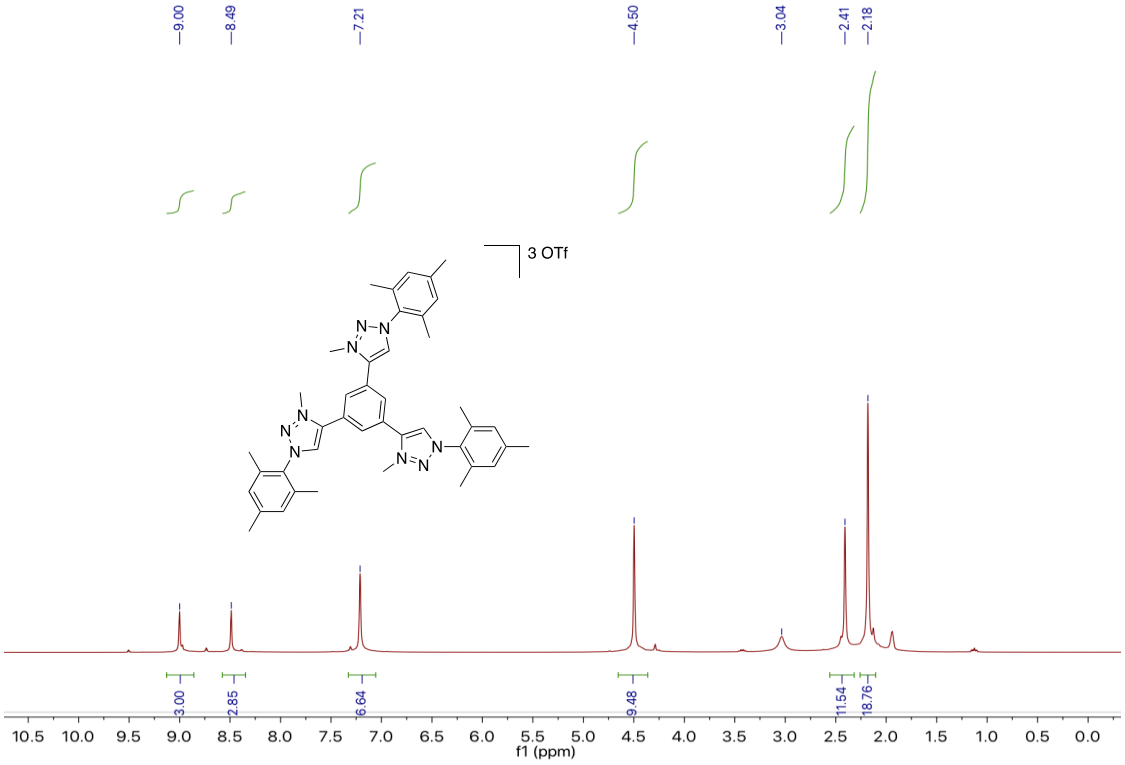

Figure S3. ^{1}H spectrum of $[H_3(\mathbf{2})](OTf)_3$ in CD_3CN

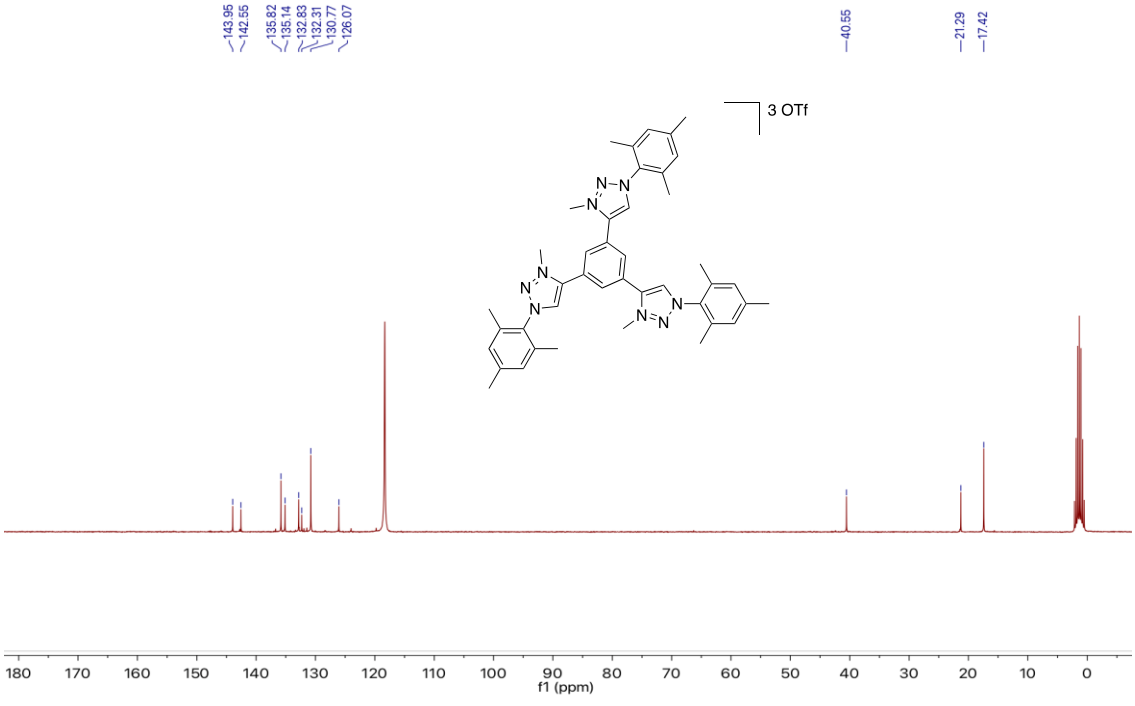

Figure S4. ^{13}C spectrum of $[H_3(\mathbf{2})](OTf)_3$ in CD_3CN

2.3. ^{1}H and ^{13}C NMR spectra of $[H_3(\mathbf{2})](Cl)_3$ in CD_2Cl_2

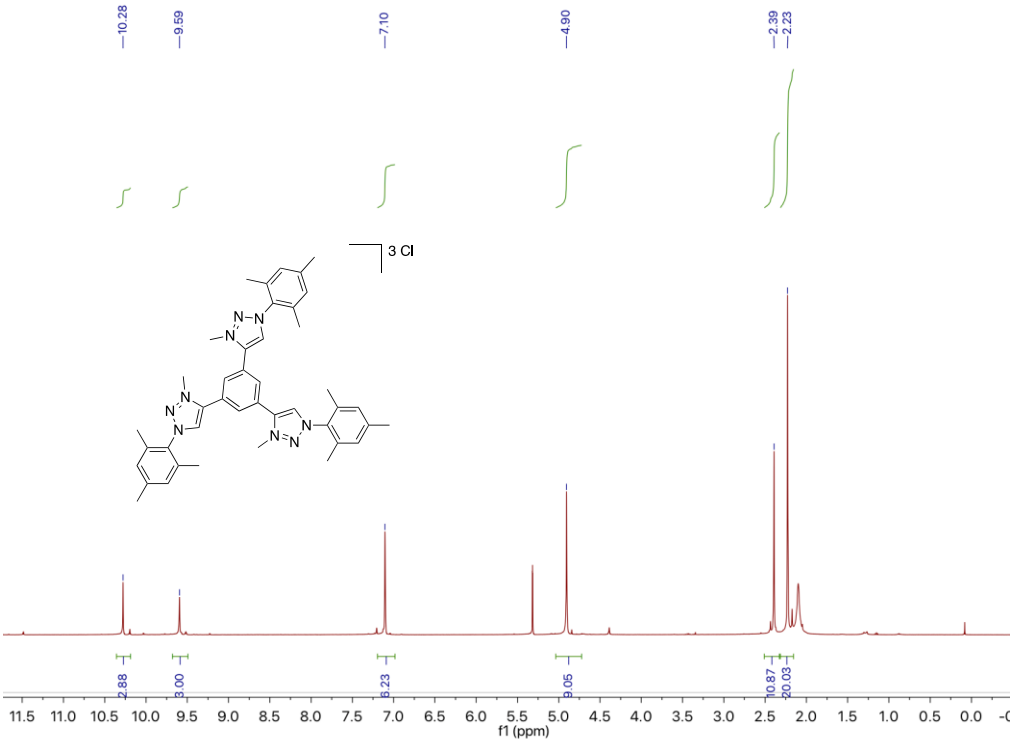

Figure S5. ^{1}H spectrum of $[H_3(\mathbf{2})](Cl)_3$ in CD_2Cl_2

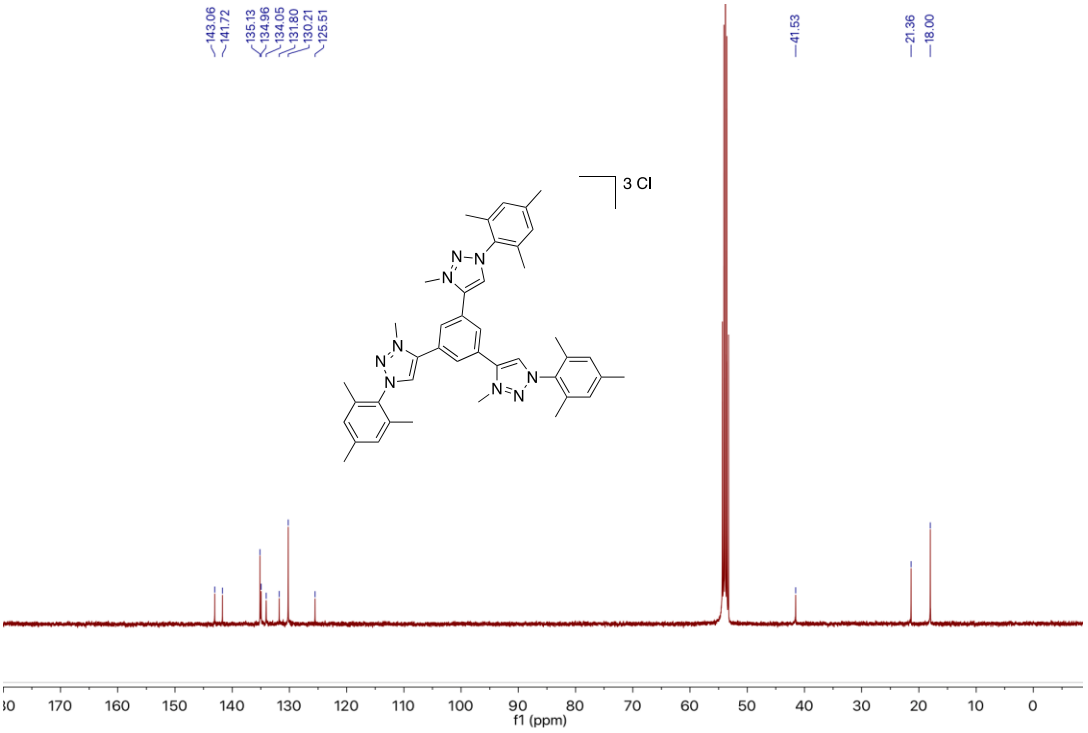

Figure S6. ^{13}C spectrum of $[H_3(\mathbf{2})](Cl)_3$ in CD_2Cl_2

2.4. ^{1}H and ^{13}C NMR spectra of $[H_3(\mathbf{2})](BF_4)_3$ in CD_3CN

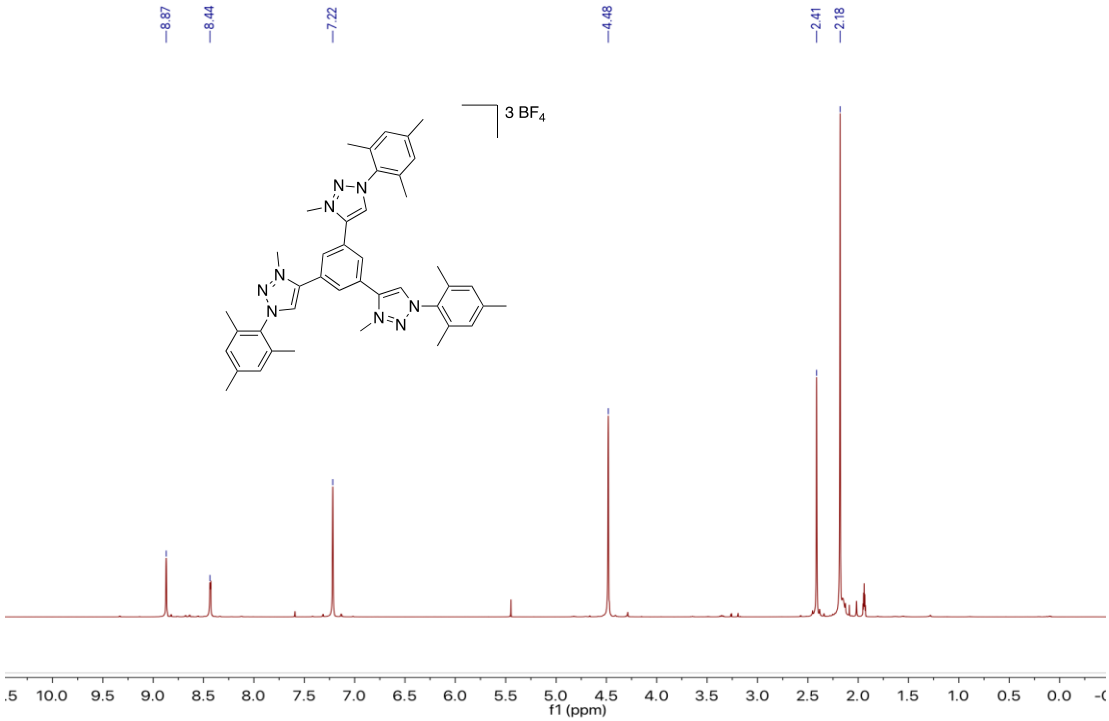

Figure S7. ^{1}H spectrum of $[H_3(\mathbf{2})](BF_4)_3$ in CD_3CN

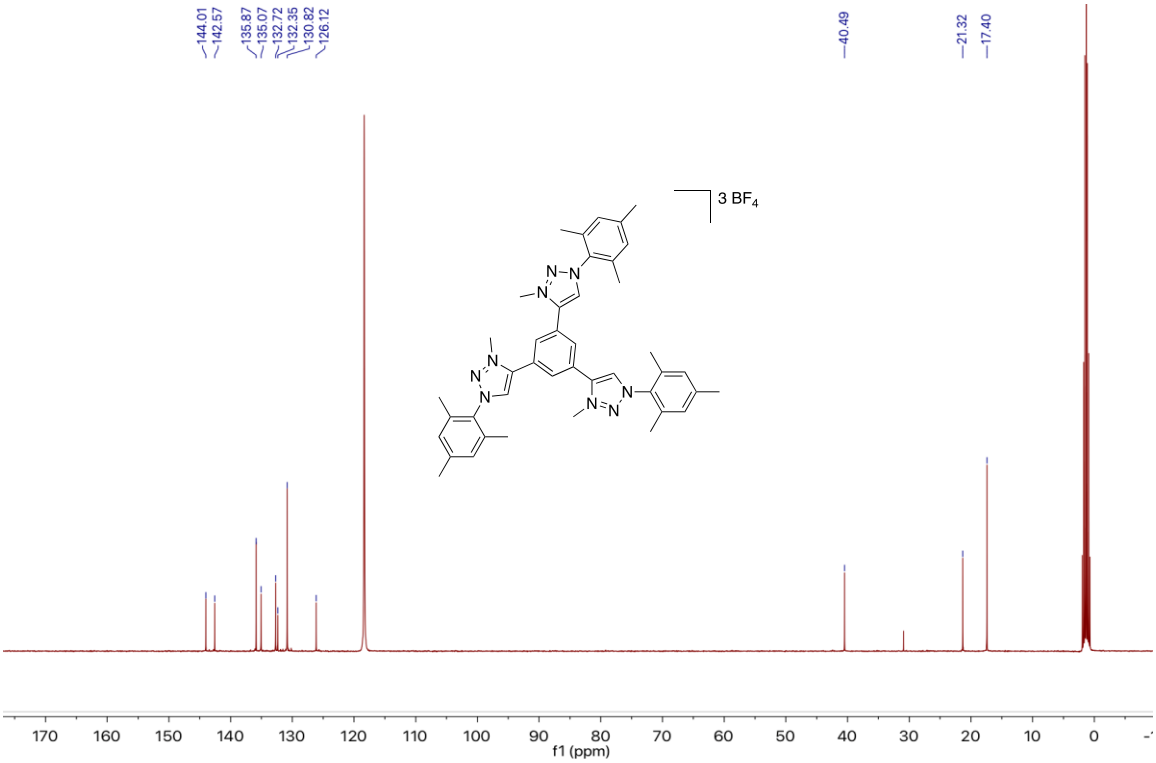

Figure S8. ^{13}C spectrum of $[H_3(\mathbf{2})](BF_4)_3$ in CD_3CN

2.5. ^{1}H and ^{13}C NMR spectra of $[Ag_3(\mathbf{2})_2](Cl)_3$ in CD_2Cl_2

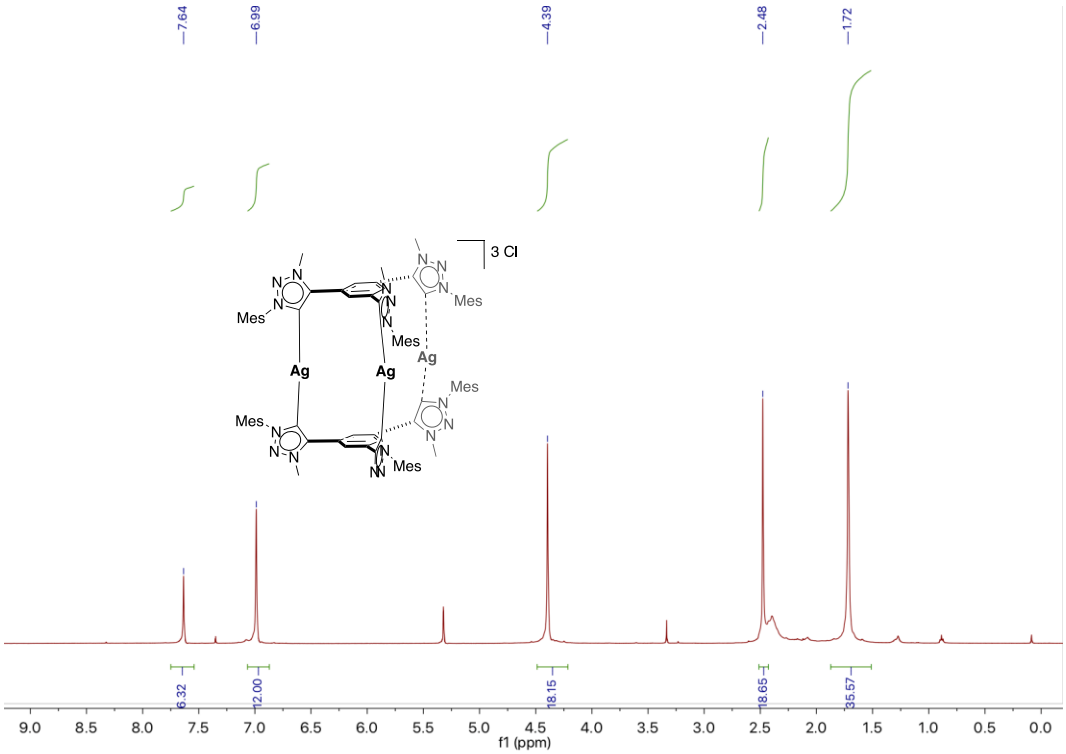

Figure S9. ^{1}H spectrum of $[Ag_3(\mathbf{2})_2](Cl)_3$ in CD_2Cl_2

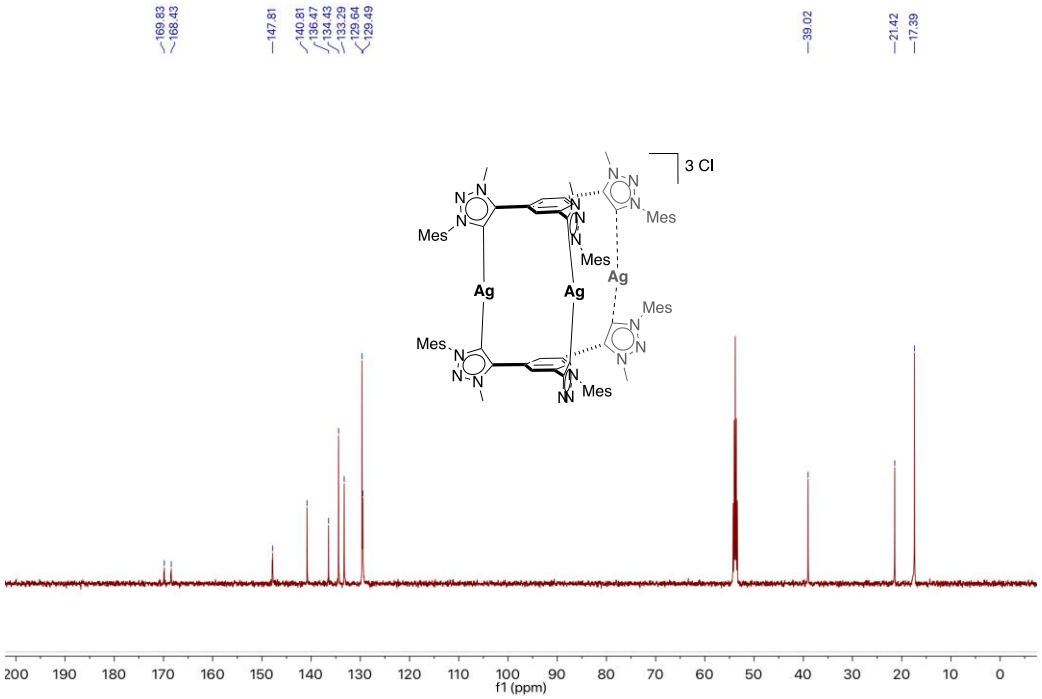

Figure S10. ^{13}C spectrum of $[Ag_3(\mathbf{2})_2](Cl)_3$ in CD_2Cl_2

2.6. ^{1}H NMR spectra in CD_3CN and ^{13}C NMR spectra in CD_2Cl_2 of $[Ag_3(\mathbf{2})_2](BF_4)_3$

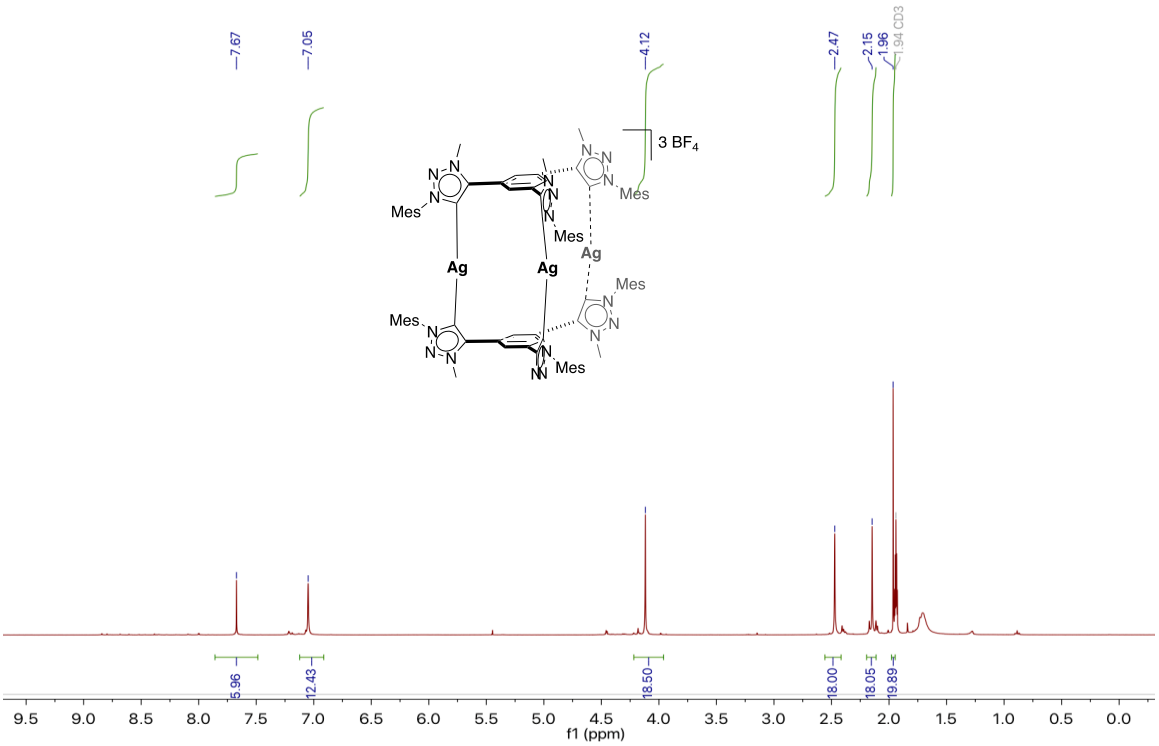

Figure S11. ^{1}H spectrum of of $[Ag_3(\mathbf{2})_2](BF_4)_3$ in CD_3CN

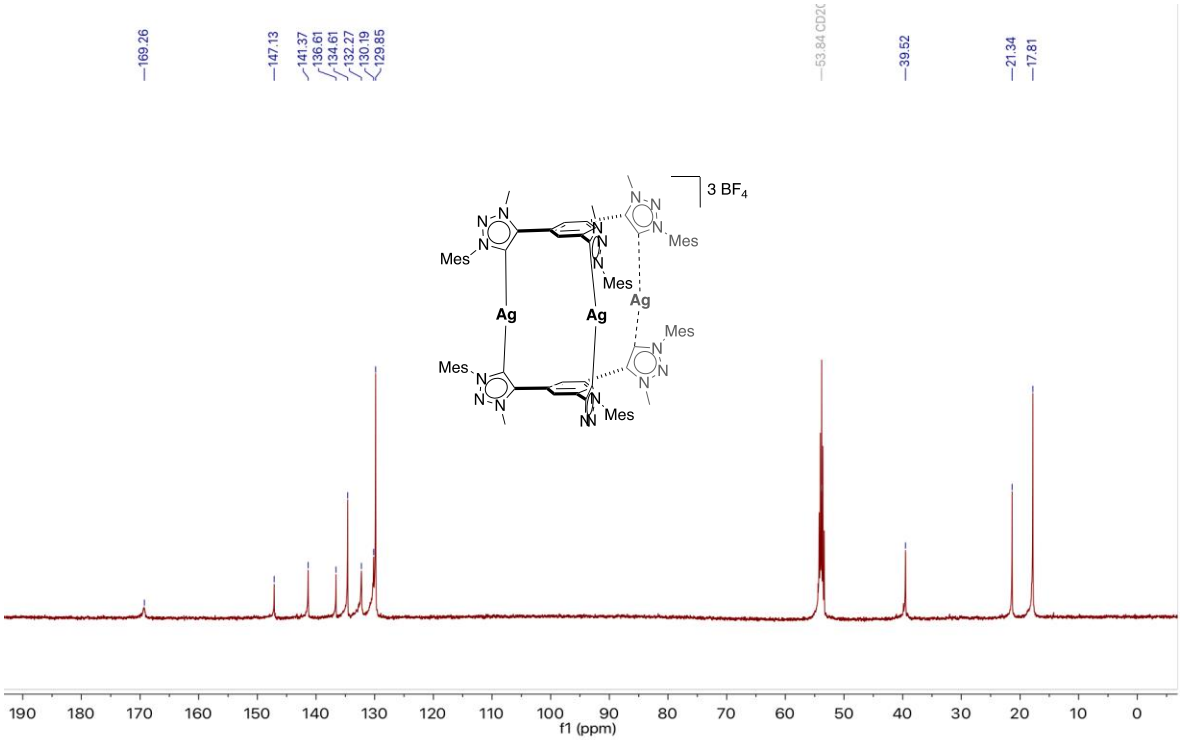

Figure S12. ^{13}C spectrum of of $[Ag_3(\mathbf{2})_2](BF_4)_3$ in CD_2Cl_2

2.7. ^{1}H and ^{13}C NMR spectra of $[Au_3(\mathbf{2})_2](Cl)_3$ in a mixture of CD_2Cl_2 and $CDCl_3$

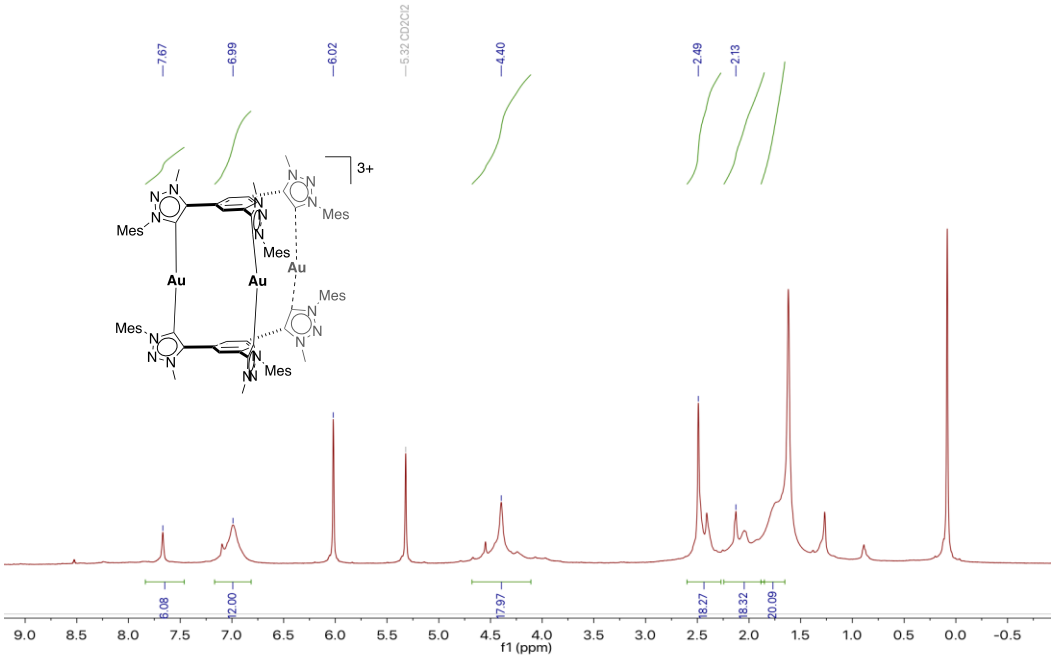

Figure S13. ^{1}H spectrum of $[Au_3(\mathbf{2})_2](Cl)_3$ in CD_2Cl_2

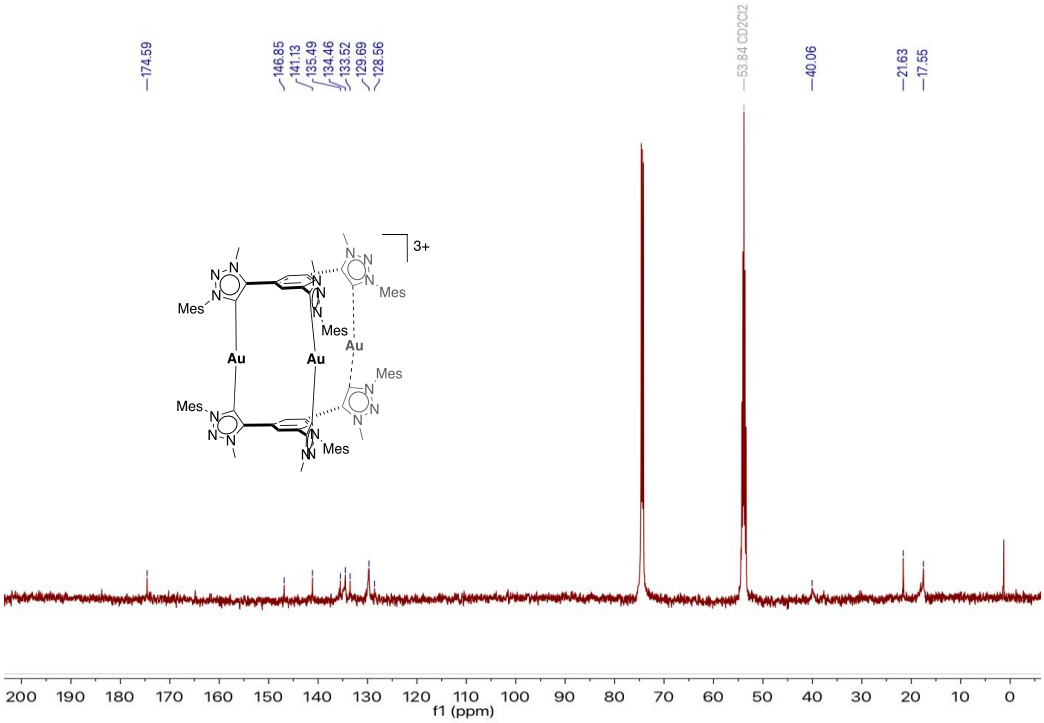

Figure S14. ^{13}C spectrum of $[Au_3(\mathbf{2})_2](Cl)_3$ in $CDCl_3$

S3. Titration Experiments:

The recognition of several anions of tetrabutylammonium salts $[NBu_4]^+X^-$ with (X^- = Cl, Br, I, $C_7H_{10}SO_3^-$ and $C_6H_5CO_2^-$) using $[H_3(\mathbf{2})](OTf)_3$ as a guest was determined by ^{1}HNMR spectroscopy in CD_3CN at 25ºC. The upfield shifts of the C(5) proton of the triazolium ring (**Ha**) along with the C-H of the central benzene (**Hb**) indicates that there is complexation between $[H_3(\mathbf{2})](OTf)_3$ and the different anions (Cl^-, Br^-, I^-, $C_7H_{10}SO_3^-$ and $C_6H_5CO_2^-$) as $[NBu_4]^+$ salts.

3.1. Chloride titration

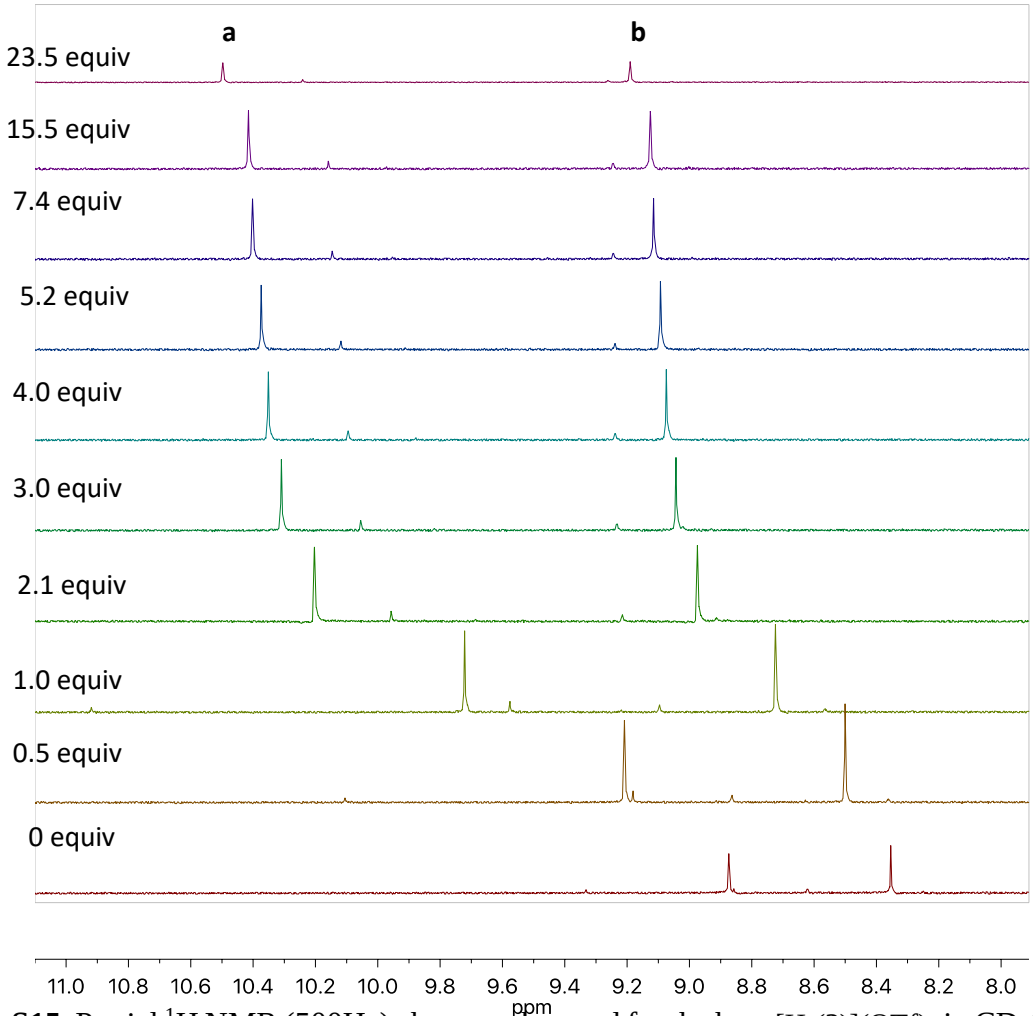

Figure S15. Partial ^{1}H NMR (500Hz) changes observed for the host $[H_3(\mathbf{2})](OTf)_3$ in CD_3CN during the addition of $[NBu_4]^+Cl^-$.

[H_3**(2)**(OTf)] **(M)**	**Equiv. [NBu_4Cl]**	**δa (ppm)**	**δb (ppm)**	**Δδa**	**Δδb**	**[NBu_4Cl] (M)**
1.99E-03	0.0	8.87	8.35	0	0	0
1.99E-03	0.2	8.89	8.42	0.02	0.07	3.21E-04
1.99E-03	0.3	9.02	8.5	0.15	0.15	6.41E-04
1.98E-03	0.5	9.21	8.58	0.34	0.23	9.58E-04
1.97E-03	0.6	9.4	8.67	0.53	0.32	1.27E-03
1.97E-03	0.8	9.59	8.72	0.72	0.37	1.59E-03
1.96E-03	1.0	9.72	8.78	0.85	0.43	1.90E-03
1.95E-03	1.1	9.84	8.83	0.97	0.48	2.21E-03
1.95E-03	1.3	9.93	8.87	1.06	0.52	2.51E-03
1.94E-03	1.5	10.02	8.9	1.15	0.55	2.82E-03
1.94E-03	1.6	10.08	8.93	1.21	0.58	3.12E-03
1.93E-03	1.8	10.13	8.95	1.26	0.6	3.42E-03
1.92E-03	1.9	10.17	8.97	1.3	0.62	3.72E-03
1.92E-03	2.1	10.2	8.99	1.33	0.64	4.02E-03
1.91E-03	2.3	10.23	9.01	1.36	0.66	4.31E-03
1.90E-03	2.4	10.25	9.02	1.38	0.67	4.61E-03
1.90E-03	2.6	10.27	9.03	1.4	0.68	4.90E-03
1.89E-03	2.7	10.29	9.04	1.42	0.69	5.19E-03
1.89E-03	2.9	10.3	9.04	1.43	0.69	5.48E-03
1.88E-03	3.1	10.31	9.05	1.44	0.7	5.76E-03
1.88E-03	3.2	10.32	9.06	1.45	0.71	6.05E-03
1.87E-03	3.4	10.33	9.06	1.46	0.71	6.33E-03
1.86E-03	3.5	10.34	9.07	1.47	0.72	6.61E-03
1.86E-03	3.7	10.34	9.07	1.47	0.72	6.89E-03
1.85E-03	3.9	10.35	9.07	1.48	0.72	7.17E-03
1.85E-03	4.0	10.35	9.08	1.48	0.73	7.44E-03
1.84E-03	4.2	10.36	9.08	1.49	0.73	7.72E-03
1.83E-03	4.4	10.36	9.08	1.49	0.73	7.99E-03
1.83E-03	4.5	10.36	9.09	1.49	0.74	8.26E-03
1.82E-03	4.7	10.37	9.09	1.5	0.74	8.53E-03
1.82E-03	4.8	10.37	9.09	1.5	0.74	8.80E-03
1.81E-03	5.2	10.38	9.1	1.51	0.75	9.33E-03
1.80E-03	5.5	10.39	9.1	1.52	0.75	9.85E-03
1.78E-03	6.0	10.39	9.11	1.52	0.76	1.06E-02
1.76E-03	6.4	10.4	9.12	1.53	0.77	1.14E-02
1.73E-03	7.4	10.42	9.13	1.55	0.78	1.29E-02
1.52E-03	15.5	10.49	9.19	1.62	0.84	2.35E-02
1.43E-03	19.5	10.5	9.19	1.63	0.84	2.78E-02

1.35E-03	23.5	10.51	9.21	1.64	0.86	3.17E-02

Table S1: Data values from the titration study of $[H_3(\mathbf{2})](OTf)_3$ during the addition of $[NBu_4]^+Cl^-$

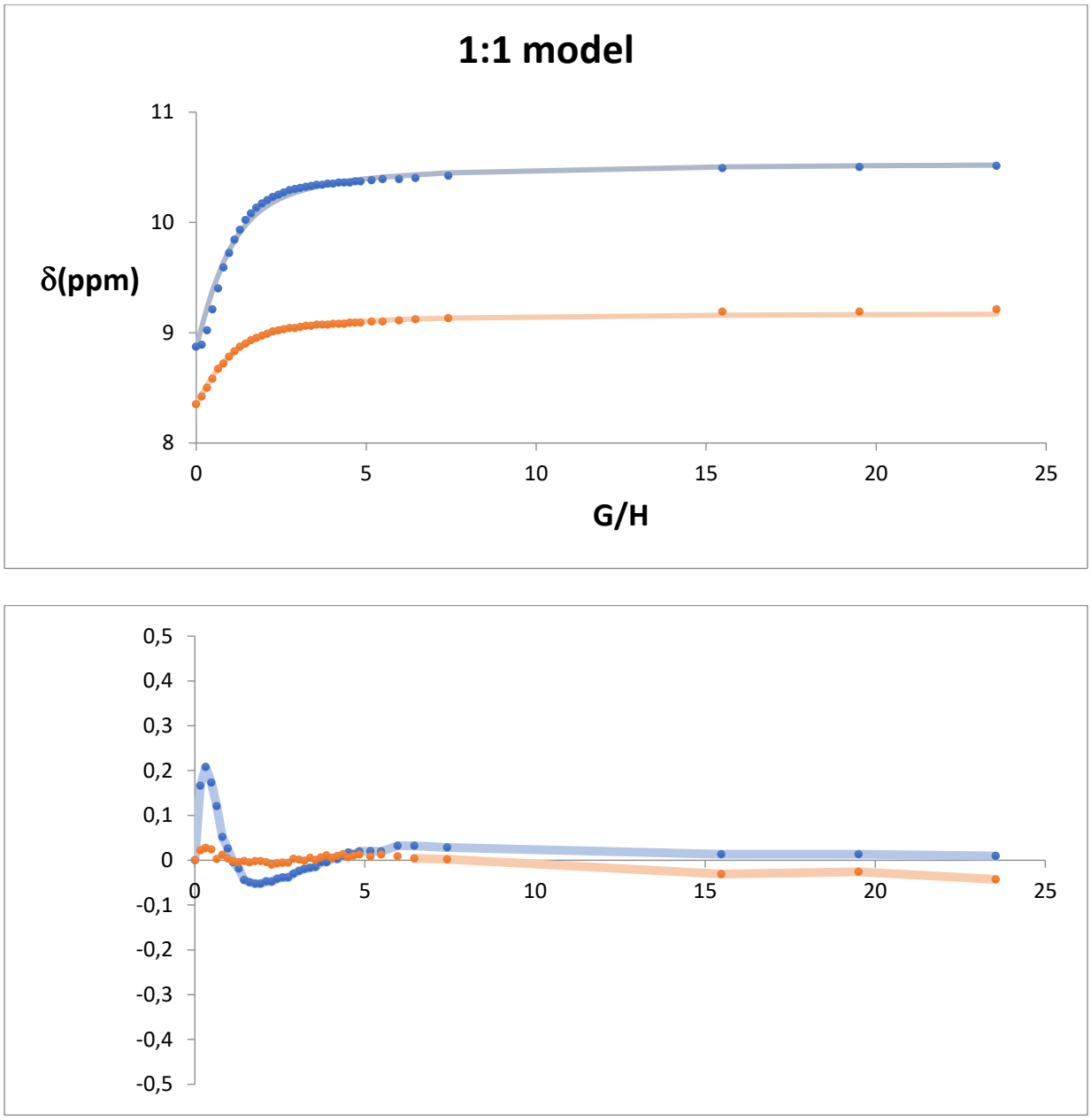

Figure S16. Representation of the δ against $[Cl^-]/[[H_3(\mathbf{2})](OTf)_3]$. Blue, orange and grey dots represent the experimental values, and solid lines represent the output fitting curve according to

the H:G model used. The best fitting corresponds to a 1:1 model (Top). This is also in accordance with the distribution of residual errors for the 1:1 model and output errors (Bottom).

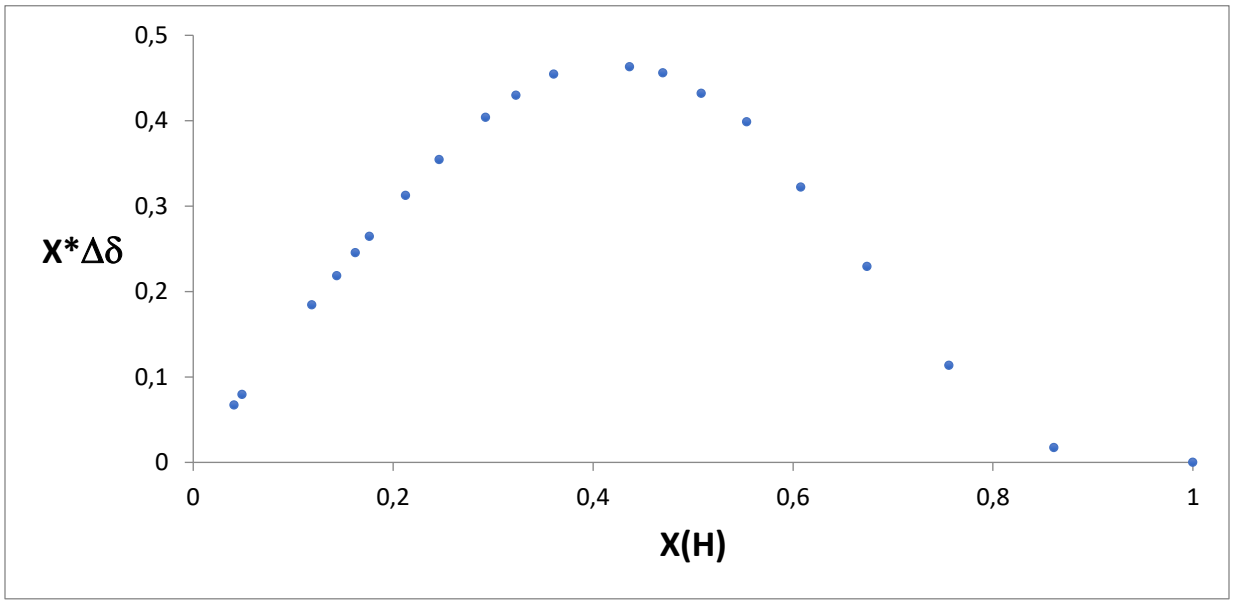

Figure S17. Job plot in CD_3CN for the interaction of $[H_3(\mathbf{2})](OTf)_3$ and $[NBu_4]^+Cl^-$ showing the 1:1 stoichiometry at 298 K.

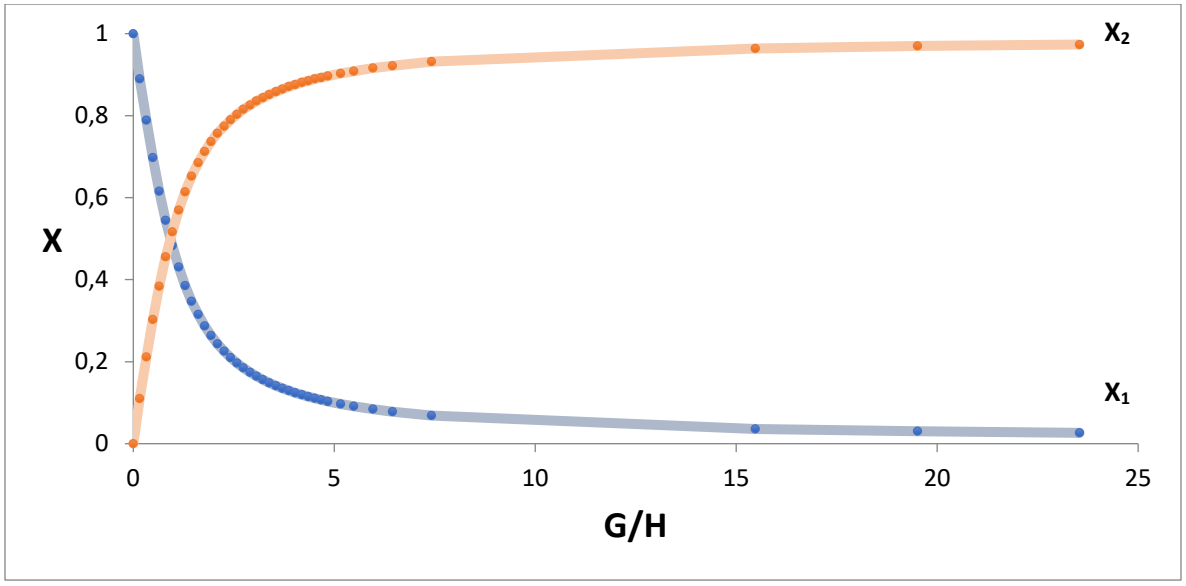

Figure S18. Speciation profile of the titration derived from by the fit of the titration data to a theoretical 1:1 binding model.

3.2. Bromide titration

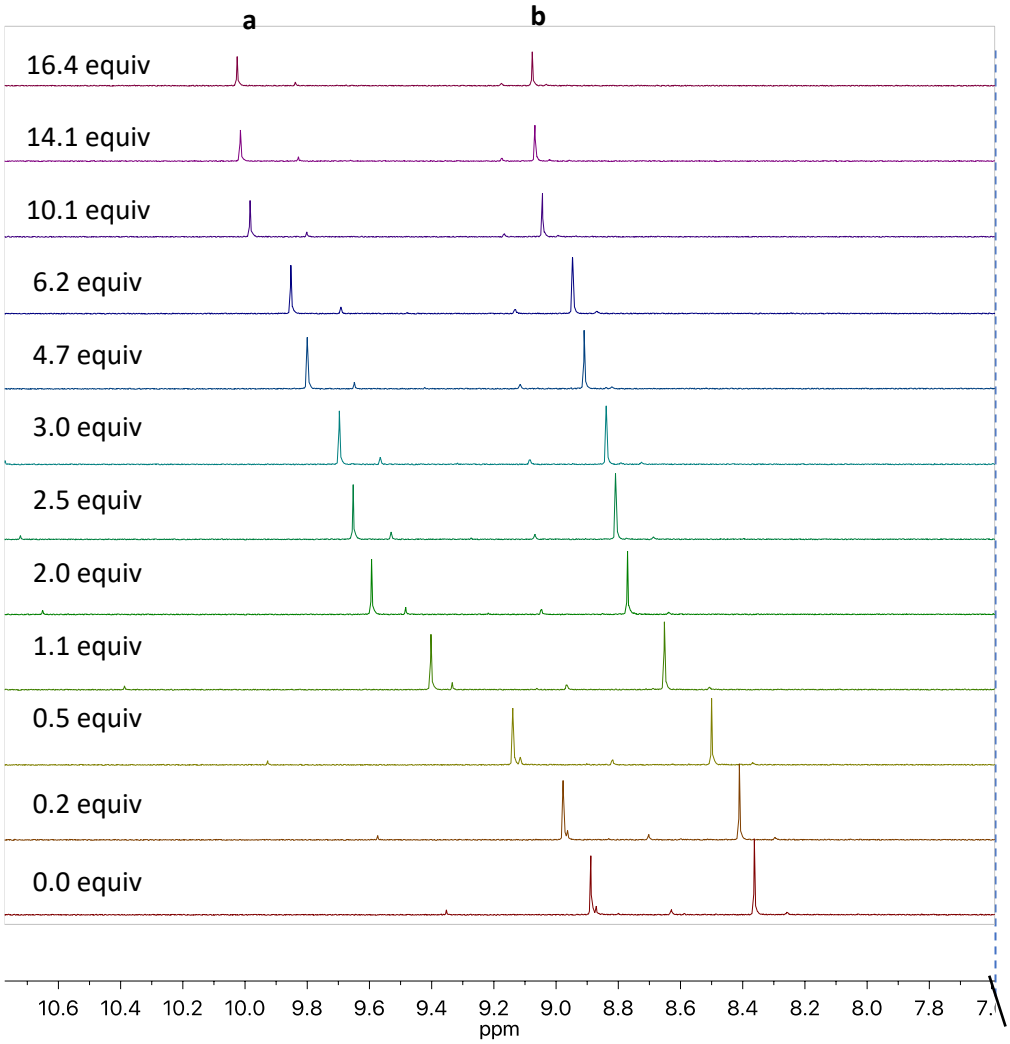

Figure S19: Partial ^{1}H NMR (500Hz) changes observed for the host $[H_3(\mathbf{2})](OTf)_3$ in CD_3CN during the addition of $[NBu_4]^+Br^-$.

[H_3(**2**)(OTf] (M)	**Equiv. [NBu_4Cl]**	**δa (ppm)**	**δb (ppm)**	**Δδa**	**Δδb**	**[NBu_4Cl] (M)**
2.00E-03	0.0	8.89	8.36	0	0	0
2.05E-03	0.2	8.98	8.41	0.09	0.05	3.20E-04
2.05E-03	0.3	9.06	8.46	0.17	0.1	6.38E-04
2.04E-03	0.5	9.14	8.46	0.25	0.1	9.53E-04
2.03E-03	0.6	9.21	8.5	0.32	0.14	1.27E-03
2.03E-03	0.8	9.29	8.54	0.4	0.18	1.58E-03
2.02E-03	0.9	9.35	8.59	0.46	0.23	1.89E-03
2.01E-03	1.1	9.4	8.62	0.51	0.26	2.20E-03
2.01E-03	1.2	9.44	8.65	0.55	0.29	2.50E-03
2.00E-03	1.4	9.48	8.68	0.59	0.32	2.80E-03
1.99E-03	1.6	9.51	8.7	0.62	0.34	3.11E-03
1.99E-03	1.7	9.54	8.72	0.65	0.36	3.41E-03
1.98E-03	1.9	9.57	8.74	0.68	0.38	3.70E-03
1.97E-03	2.0	9.59	8.76	0.7	0.4	4.00E-03
1.97E-03	2.2	9.61	8.77	0.72	0.41	4.29E-03
1.96E-03	2.3	9.64	8.78	0.75	0.42	4.59E-03
1.96E-03	2.5	9.65	8.8	0.76	0.44	4.88E-03
1.95E-03	2.6	9.67	8.81	0.78	0.45	5.16E-03
1.94E-03	2.8	9.68	8.82	0.79	0.46	5.45E-03
1.94E-03	3.0	9.7	8.83	0.81	0.47	5.74E-03
1.93E-03	3.1	9.71	8.84	0.82	0.48	6.02E-03
1.90E-03	3.9	9.76	8.85	0.87	0.49	7.41E-03
1.87E-03	4.7	9.8	8.88	0.91	0.52	8.76E-03
1.85E-03	5.5	9.83	8.91	0.94	0.55	1.01E-02
1.82E-03	6.2	9.85	8.93	0.96	0.57	1.13E-02
1.75E-03	8.2	9.95	8.95	1.06	0.59	1.43E-02
1.69E-03	10.1	9.98	9.02	1.09	0.66	1.72E-02
1.64E-03	12.1	10	9.04	1.11	0.68	1.98E-02
1.59E-03	14.0	10.01	9.06	1.12	0.7	2.22E-02
1.54E-03	16.0	10.03	9.07	1.14	0.71	2.45E-02
1.53E-03	16.4	10.05	9.08	1.16	0.72	2.50E-02

Table S2: Data values from the titration study of [H_3(**2**)]$(OTf)_3$ during the addition of $[NBu_4]^+Br^-$

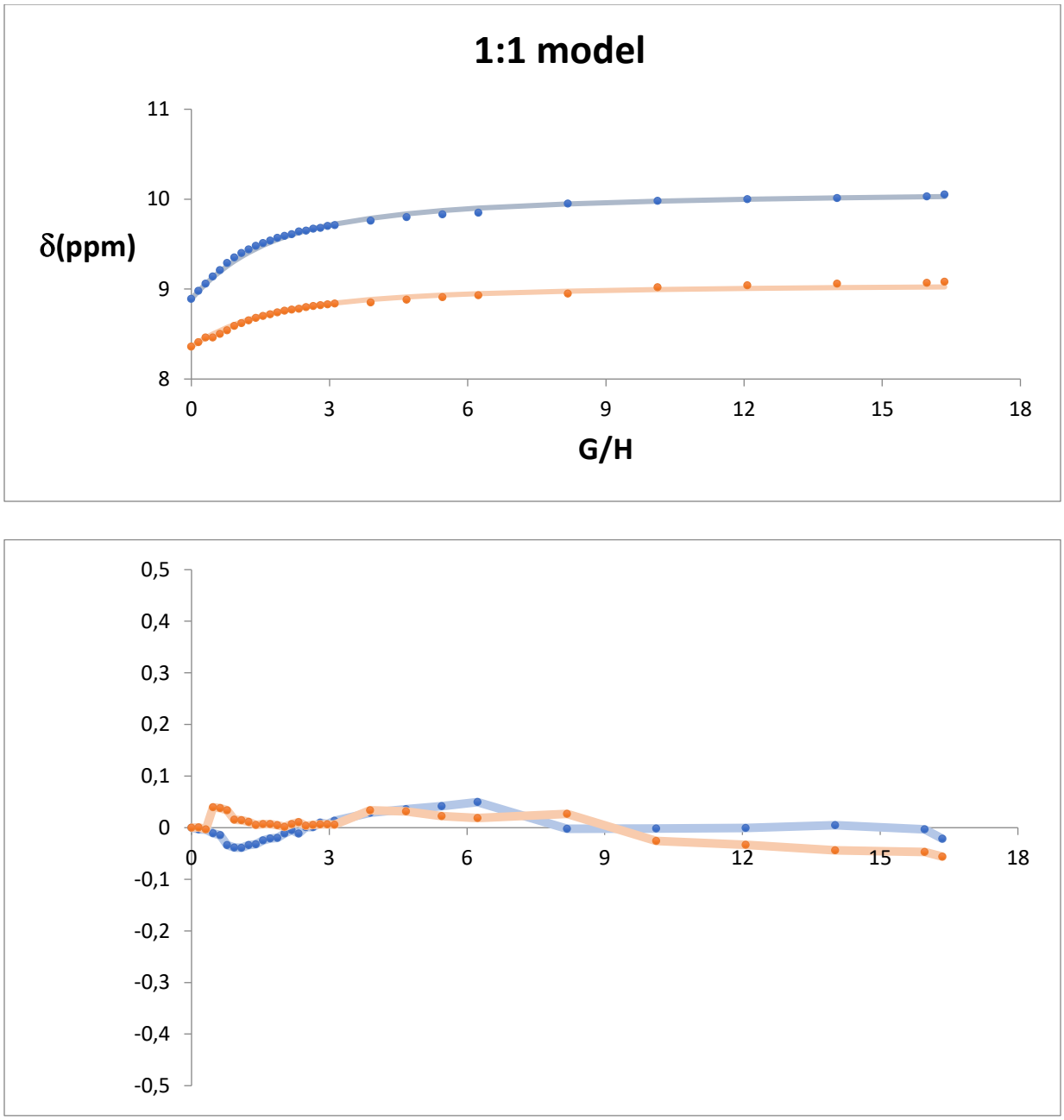

Figure S20. Representation of the δ against [Br^-]/**[**[H_3(**2**)](OTf)$_3$]. Blue, orange and grey dots represent the experimental values, and solid lines represent the output fitting curve according to the H:G model used. The best fitting corresponds to a 1:1 model. This is also in accordance with the distribution of residual errors for the 1:1 model and output errors.

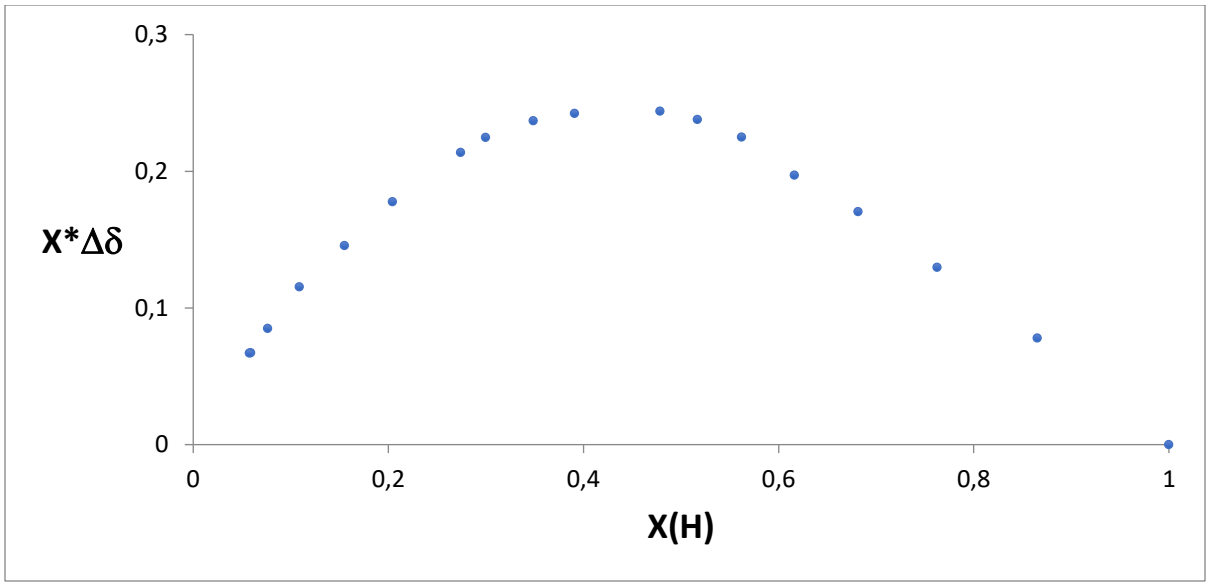

Figure S21. Job plot in CD_3CN for the interaction of $[H_3(\mathbf{2})](OTf)_3$ and $[NBu_4]^+Br^-$ showing the 1:1 stoichiometry at 298 K.

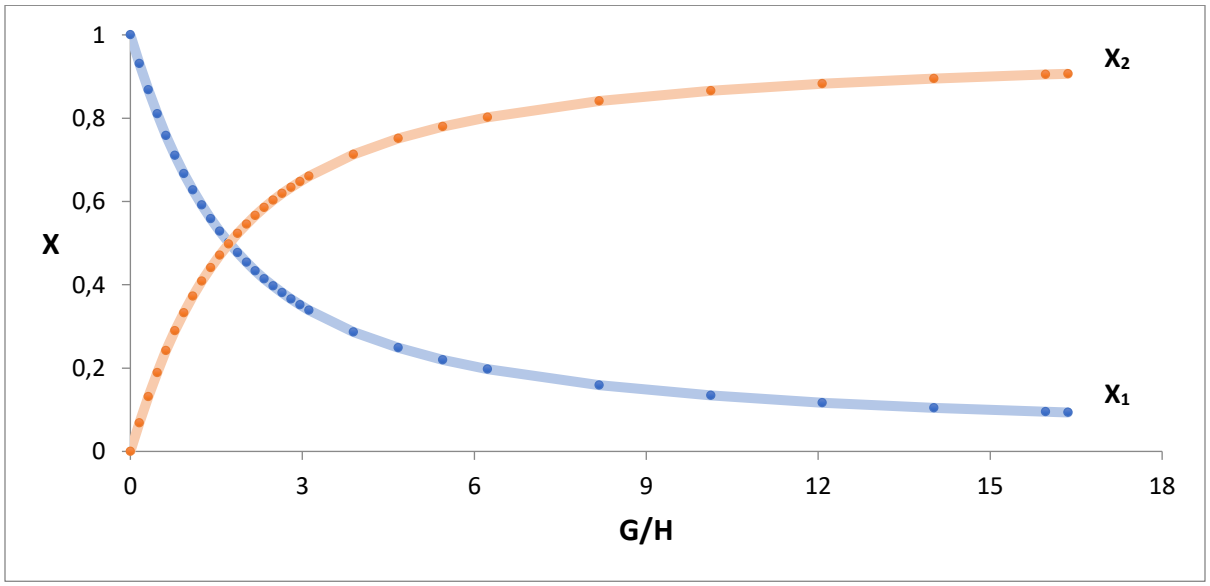

Figure S22. Speciation profile of the titration derived from by the fit of the titration data to a theoretical 1:1 binding model.

3.3 Iodide titration

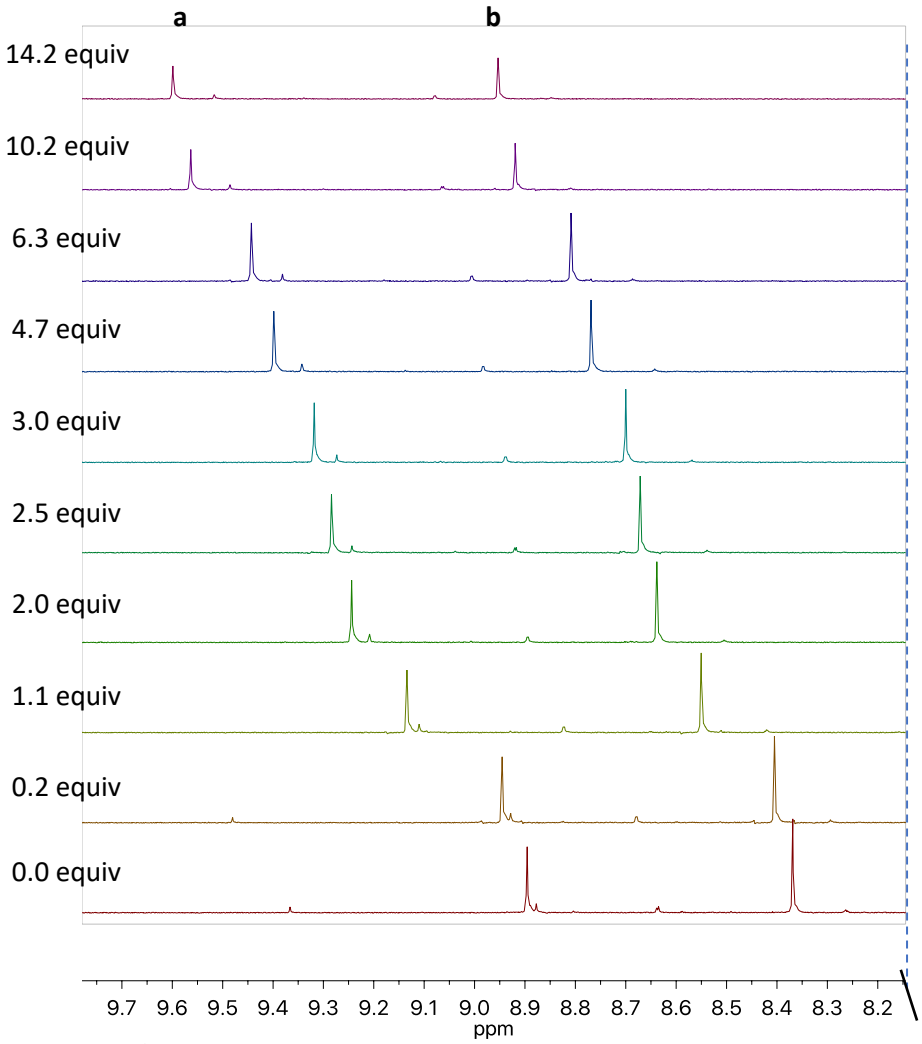

Figure S23: Partial ^{1}H NMR (500Hz) changes observed for the host $[H_3(\mathbf{2})](OTf)_3$ in CD_3CN during the addition of $[NBu_4]^+I^-$.

[H_3(**2**)(OTf] **(M)**	**Equiv. [NBu_4Cl]**	**δa (ppm)**	**δb (ppm)**	**Δδa**	**Δδb**	**[NBu_4Cl] (M)**
2.04E-03	0.0	8.89	8.37	0	0	0
2.03E-03	0.2	8.95	8.41	0.06	0.04	3.17E-04
2.03E-03	0.3	8.99	8.44	0.1	0.07	6.38E-04
2.02E-03	0.5	9.02	8.47	0.13	0.1	9.54E-04
2.01E-03	0.6	9.06	8.49	0.17	0.12	1.27E-03
2.01E-03	0.8	9.08	8.51	0.19	0.14	1.58E-03
2.00E-03	0.9	9.11	8.53	0.22	0.16	1.89E-03
1.99E-03	1.1	9.13	8.55	0.24	0.18	2.20E-03
1.99E-03	1.3	9.16	8.57	0.27	0.2	2.50E-03
1.98E-03	1.4	9.18	8.58	0.29	0.21	2.81E-03
1.98E-03	1.6	9.2	8.6	0.31	0.23	3.11E-03
1.97E-03	1.7	9.21	8.61	0.32	0.24	3.41E-03
1.96E-03	1.9	9.23	8.63	0.34	0.26	3.71E-03
1.96E-03	2.0	9.24	8.64	0.35	0.27	4.00E-03
1.95E-03	2.2	9.26	8.65	0.37	0.28	4.30E-03
1.94E-03	2.4	9.27	8.66	0.38	0.29	4.59E-03
1.94E-03	2.5	9.28	8.67	0.39	0.3	4.88E-03
1.93E-03	2.7	9.3	8.68	0.41	0.31	5.17E-03
1.93E-03	2.8	9.31	8.69	0.42	0.32	5.46E-03
1.92E-03	3.0	9.32	8.7	0.43	0.33	5.74E-03
1.91E-03	3.1	9.33	8.71	0.44	0.34	6.02E-03
1.89E-03	3.9	9.37	8.74	0.48	0.37	7.42E-03
1.86E-03	4.7	9.4	8.77	0.51	0.4	8.77E-03
1.83E-03	5.5	9.42	8.79	0.53	0.42	1.01E-02
1.80E-03	6.3	9.44	8.83	0.55	0.46	1.13E-02
1.74E-03	8.3	9.52	8.88	0.63	0.51	1.44E-02
1.68E-03	10.2	9.56	8.92	0.67	0.55	1.72E-02
1.63E-03	12.2	9.59	8.94	0.7	0.57	1.98E-02
1.57E-03	14.2	9.6	8.95	0.71	0.58	2.23E-02

Table S3: data values from the titration study of $[H_3(\mathbf{2})](OTf)_3$ during the addition of $[NBu_4]^+I^-$

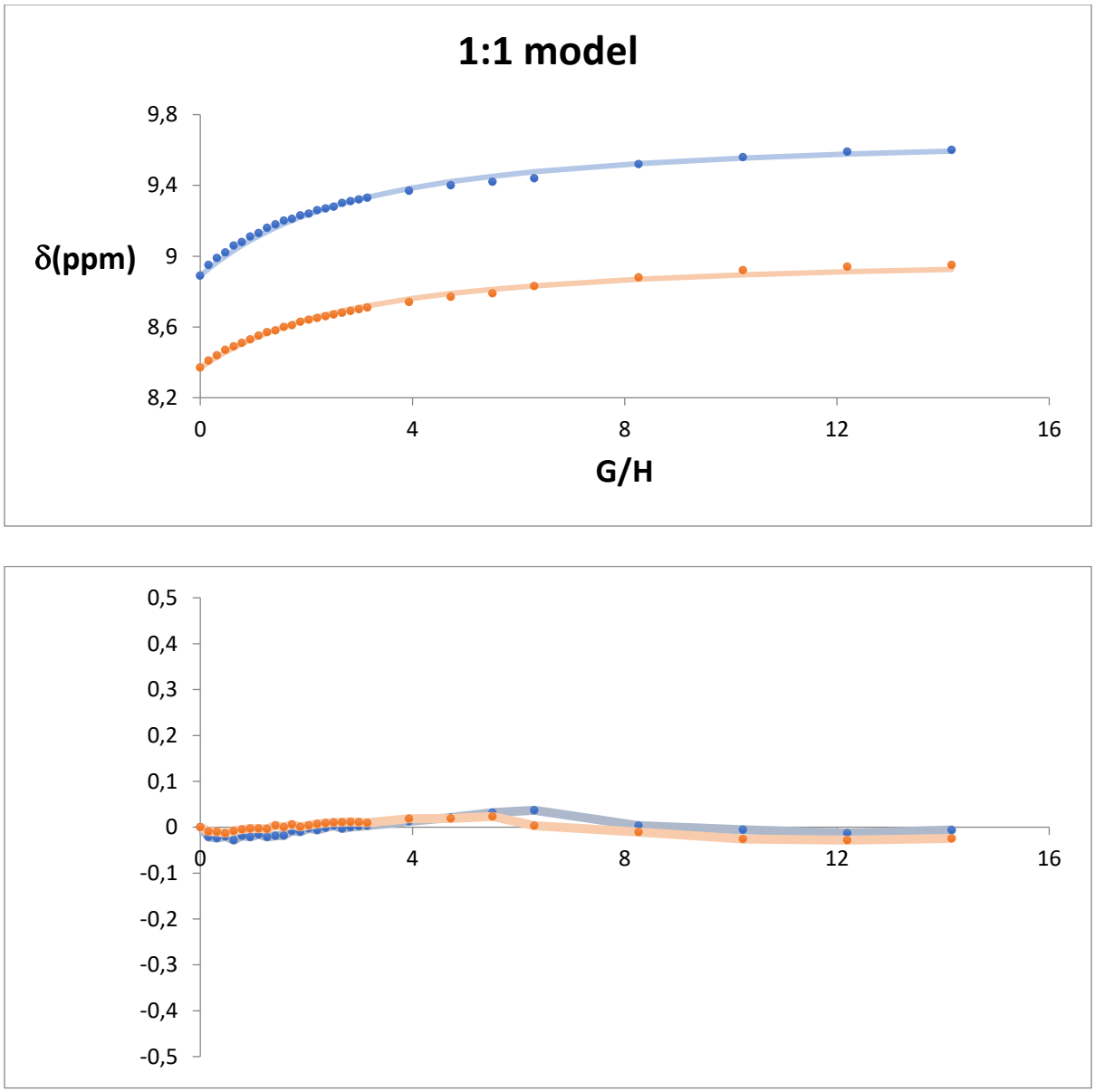

Figure S24. Representation of the δ against $[I^-]$/**[**$[H_3(\mathbf{2})](OTf)_3$]. Blue and orange dots represent the experimental values, and solid lines represent the output fitting curve according to the H:G model used. The best fitting corresponds to a 1:1 model. This is also in accordance with the distribution of residual errors for the 1:1 model and output errors.

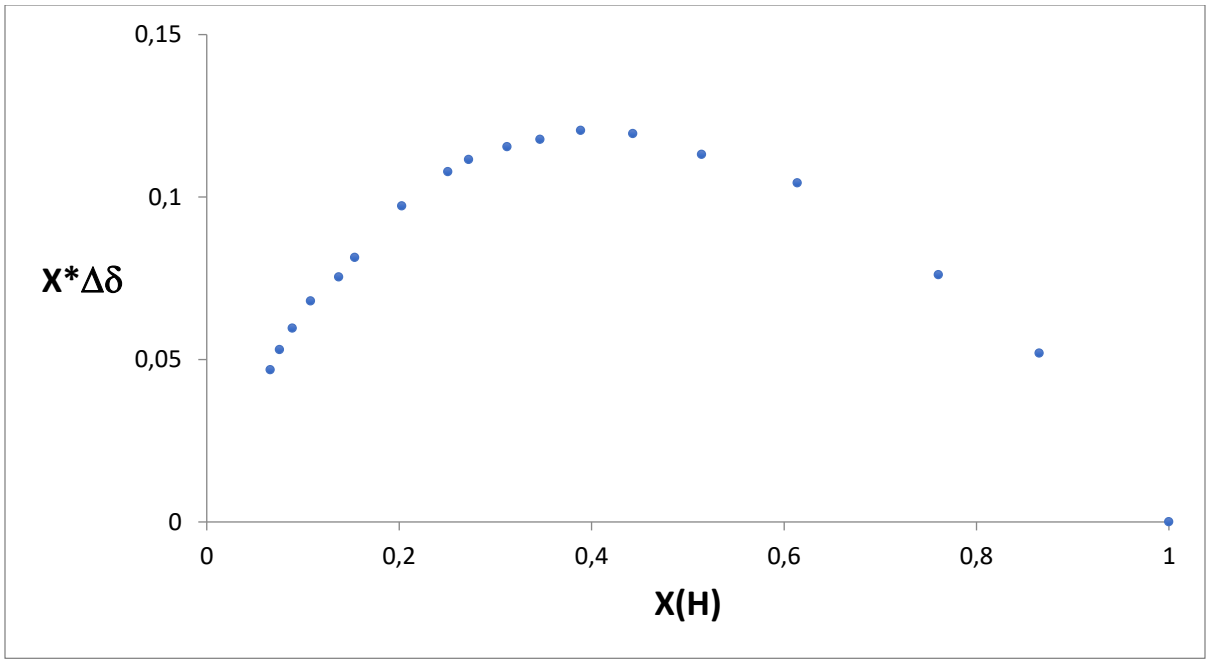

Figure S25. Job plot in CD_3CN for the interaction of $[H_3(\mathbf{2})](OTf)_3$ and $[NBu_4]^+I^-$ showing the 1:1 stoichiometry at 298 K.

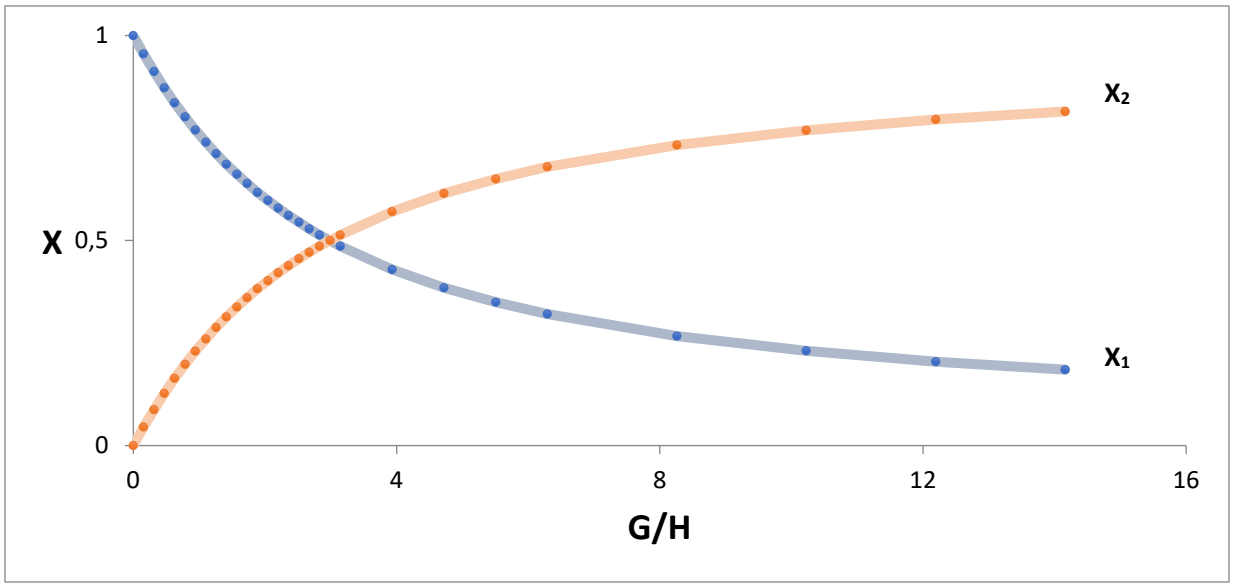

Figure S26. Speciation profile of the titration derived from by the fit of the titration data to a theoretical 1:1 binding model.

3.4 *p*-Toluensulfonate titration

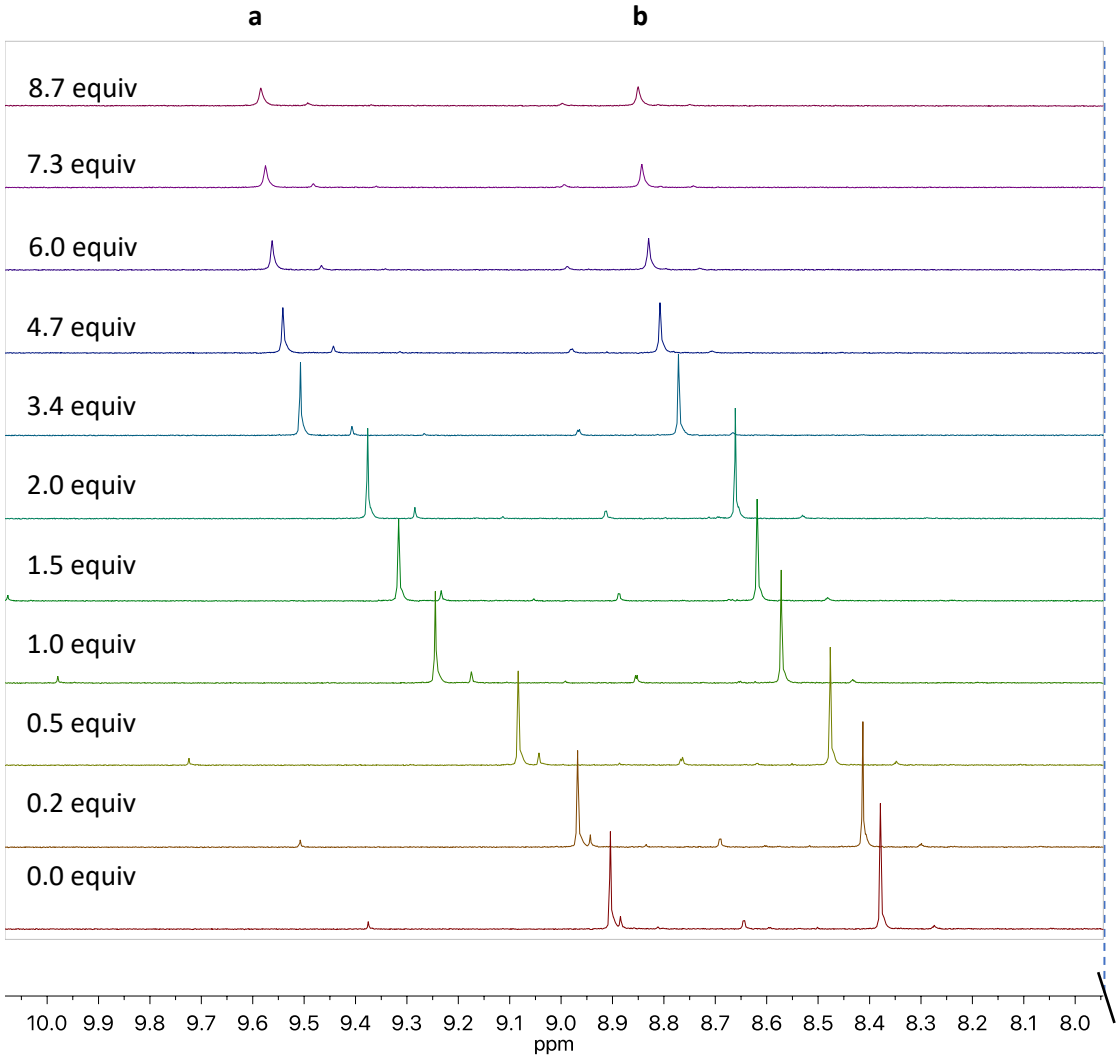

Figure S27: Partial ^{1}H NMR (500Hz) changes observed for the host $[H_3(\mathbf{2})](OTf)_3$ in CD_3CN during the addition of $[NBu_4]^+C_7H_{10}SO_3^-$.

[H_3(**2**)(OTf] (M)	**Equiv. [NBu_4Cl]**	**δa (ppm)**	**δb (ppm)**	**Δδa**	**Δδb**	**[NBu_4Cl] (M)**
3.24E-03	0.0	8.9	8.38	0	0	0
3.23E-03	0.1	8.92	8.39	0.02	0.01	3.19E-04
3.22E-03	0.2	8.97	8.41	0.07	0.03	6.76E-04
3.21E-03	0.3	9.01	8.43	0.11	0.05	1.01E-03
3.20E-03	0.4	9.05	8.46	0.15	0.08	1.34E-03
3.19E-03	0.5	9.08	8.48	0.18	0.1	1.67E-03
3.18E-03	0.6	9.12	8.5	0.22	0.12	2.00E-03
3.17E-03	0.7	9.15	8.51	0.25	0.13	2.33E-03
3.16E-03	0.8	9.19	8.54	0.29	0.16	2.65E-03
3.15E-03	0.9	9.22	8.56	0.32	0.18	2.97E-03
3.14E-03	1.0	9.25	8.57	0.35	0.19	3.29E-03
3.13E-03	1.2	9.26	8.58	0.36	0.2	3.61E-03
3.12E-03	1.3	9.28	8.6	0.38	0.22	3.93E-03
3.11E-03	1.4	9.3	8.61	0.4	0.23	4.24E-03
3.10E-03	1.5	9.32	8.62	0.42	0.24	4.55E-03
3.09E-03	1.6	9.33	8.63	0.43	0.25	4.86E-03
3.08E-03	1.7	9.34	8.64	0.44	0.26	5.17E-03
3.07E-03	1.8	9.36	8.65	0.46	0.27	5.47E-03
3.06E-03	1.9	9.37	8.65	0.47	0.27	5.78E-03
3.05E-03	2.0	9.38	8.66	0.48	0.28	6.08E-03
3.04E-03	2.1	9.39	8.67	0.49	0.29	6.38E-03
2.93E-03	3.4	9.51	8.77	0.61	0.39	9.98E-03
2.82E-03	4.7	9.54	8.81	0.64	0.43	1.33E-02
2.72E-03	6.0	9.56	8.83	0.66	0.45	1.64E-02
2.63E-03	7.3	9.57	8.84	0.67	0.46	1.93E-02
2.54E-03	8.7	9.58	8.85	0.68	0.47	2.20E-02

Table S4: Data values from the titration study of $[H_3(\mathbf{2})](OTf)_3$ during the addition of $[NBu_4]^+C_7H_{10}SO_3^-$

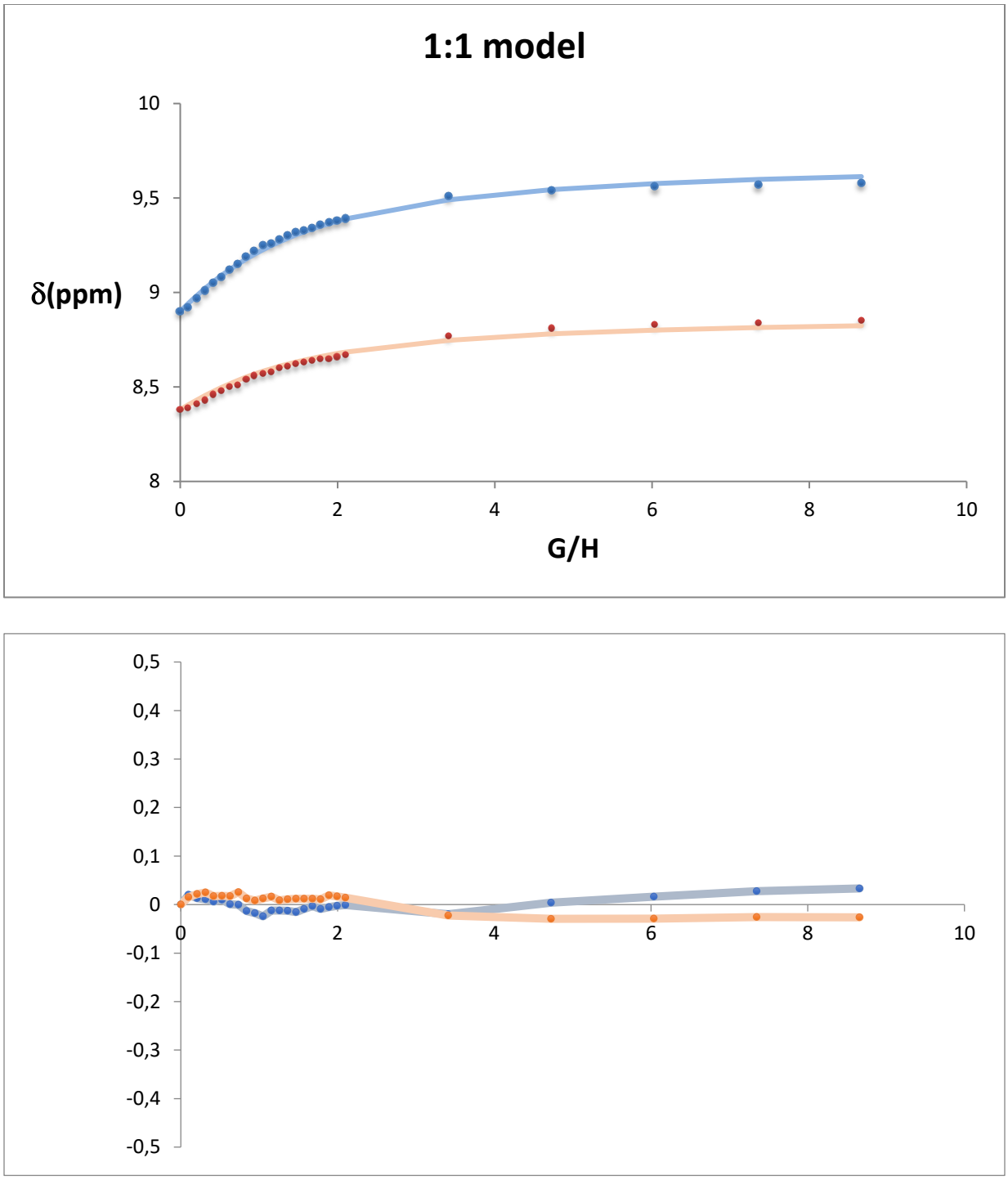

Figure S28. Representation of the δ against $[C_7H_{10}SO_3^-]/[H_3(\mathbf{2})](OTf)_3]$. Blue, orange and grey dots represent the experimental values, and solid lines represent the output fitting curve according to the H:G model used. The best fitting corresponds to a 1:1 model. This is also in accordance with the distribution of residual errors for the 1:1 model and output errors.

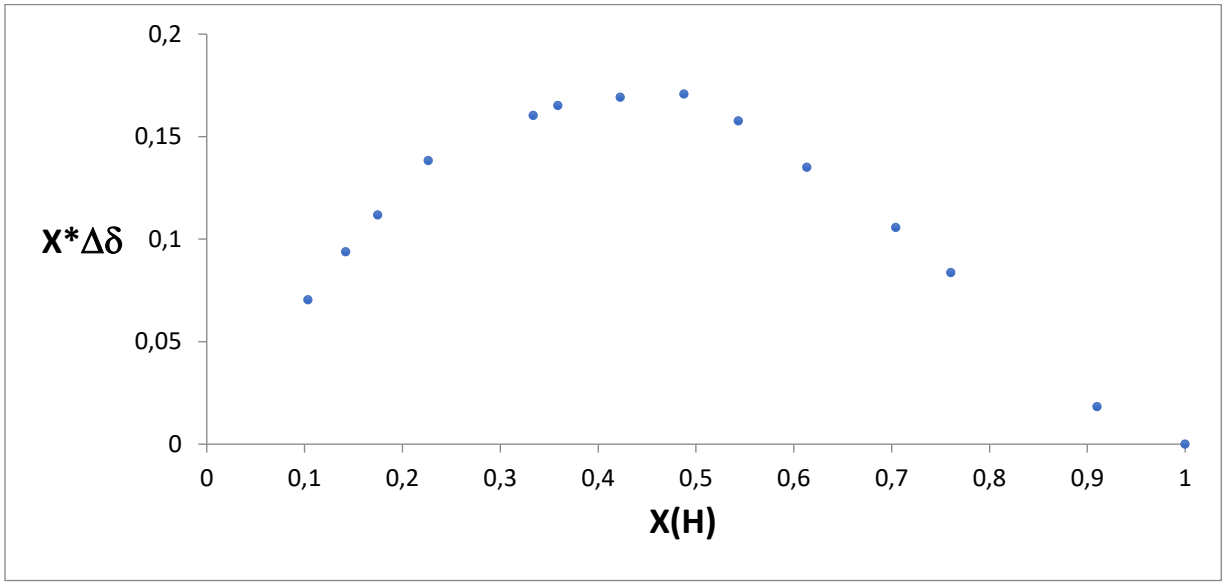

Figure S29. Job plot in CD_3CN for the interaction of $[H_3(\mathbf{2})](OTf)_3$ and $[NBu_4]^+C_7H_{10}SO_3^-$ showing the 1:1 stoichiometry at 298 K.

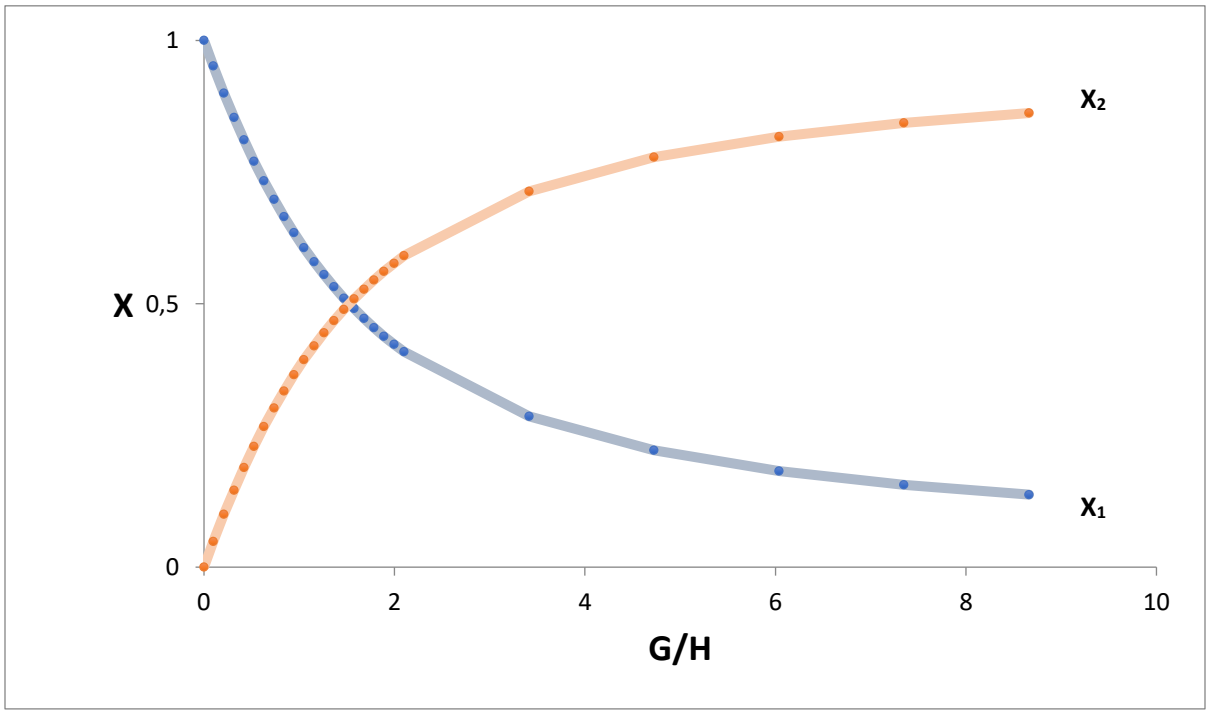

Figure S30. Speciation profile of the titration derived from by the fit of the titration data to a theoretical 1:1 binding model.

3.5 Benzoate titration

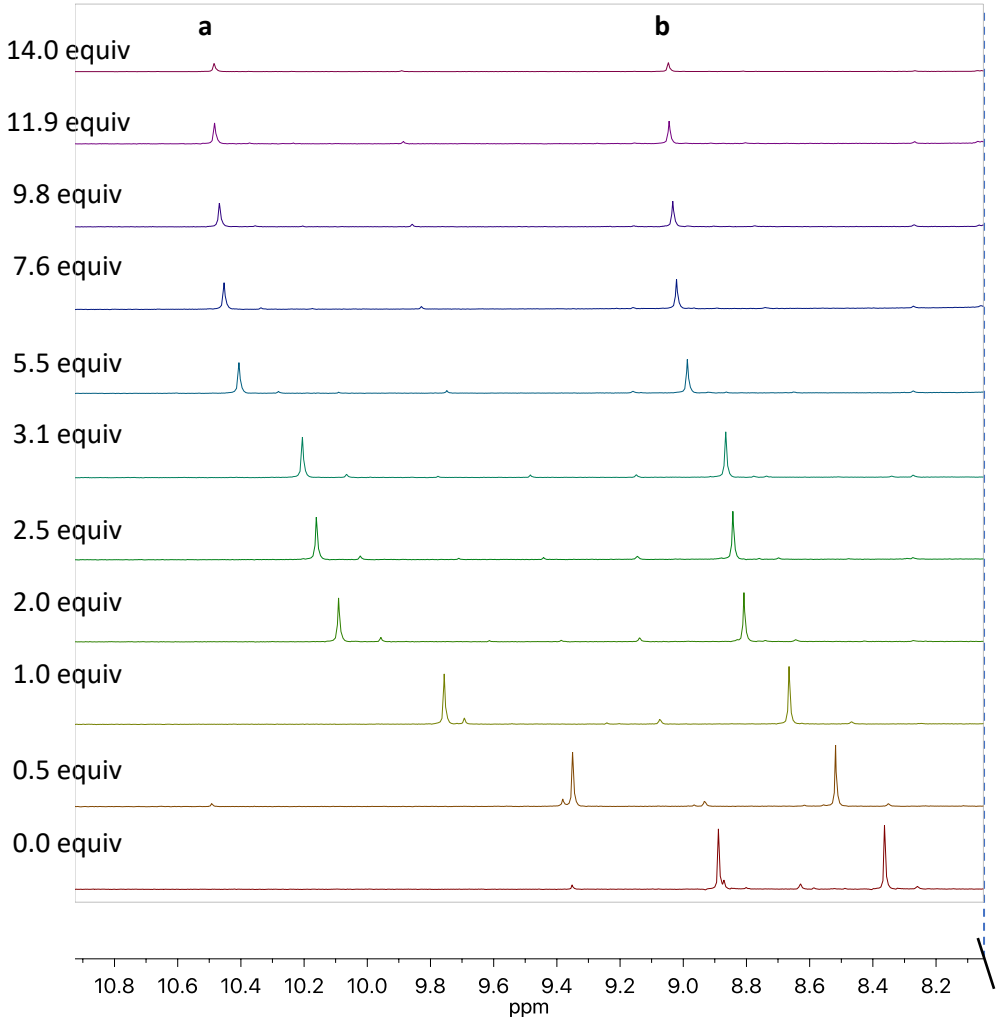

Figure S31: ^{1}H NMR (500Hz) changes observed for the host $[H_3(\mathbf{2})](OTf)_3$ in CD_3CN during the addition of $[NBu_4]^+C_6H_5CO_2^-$.

[H_3(**2**)(OTf] (M)	**Equiv. [NBu_4Cl]**	**δa (ppm)**	**δb (ppm)**	**Δδa**	**Δδb**	**[NBu_4Cl] (M)**
1.92E-03	0	8.89	8.36	0	0	0
1.91E-03	0.2	8.93	8.38	0.04	0.02	3.21E-04
1.91E-03	0.3	9.15	8.45	0.26	0.09	6.47E-04
1.90E-03	0.5	9.35	8.52	0.46	0.16	9.68E-04
1.89E-03	0.7	9.5	8.57	0.61	0.21	1.29E-03
1.89E-03	0.8	9.66	8.63	0.77	0.27	1.60E-03
1.88E-03	1.0	9.76	8.67	0.87	0.31	1.92E-03
1.88E-03	1.2	9.84	8.7	0.95	0.34	2.23E-03
1.87E-03	1.4	9.91	8.73	1.02	0.37	2.54E-03
1.86E-03	1.5	9.97	8.75	1.08	0.39	2.85E-03
1.86E-03	1.7	10.05	8.79	1.16	0.43	3.15E-03
1.85E-03	1.9	10.09	8.81	1.2	0.45	3.46E-03
1.85E-03	2.0	10.12	8.82	1.23	0.46	3.76E-03
1.84E-03	2.2	10.14	8.83	1.25	0.47	4.06E-03
1.83E-03	2.4	10.16	8.84	1.27	0.48	4.36E-03
1.83E-03	2.5	10.18	8.85	1.29	0.49	4.65E-03
1.82E-03	2.7	10.2	8.87	1.31	0.51	4.95E-03
1.82E-03	2.9	10.22	8.87	1.33	0.51	5.24E-03
1.81E-03	3.1	10.23	8.88	1.34	0.52	5.53E-03
1.81E-03	3.2	10.24	8.89	1.35	0.53	5.82E-03
1.80E-03	3.4	10.25	8.9	1.36	0.54	6.11E-03
1.73E-03	5.5	10.43	9.01	1.54	0.65	9.55E-03
1.67E-03	7.6	10.47	9.04	1.58	0.68	1.27E-02
1.61E-03	9.8	10.49	9.05	1.6	0.69	1.57E-02
1.56E-03	11.9	10.5	9.07	1.61	0.71	1.85E-02
1.51E-03	14.0	10.5	9.07	1.61	0.71	2.11E-02

Table S5: Data values from the titration study of $[H_3(\mathbf{2})](OTf)_3$ during the addition of and $[NBu_4]^+C_6H_5CO_2^-$.

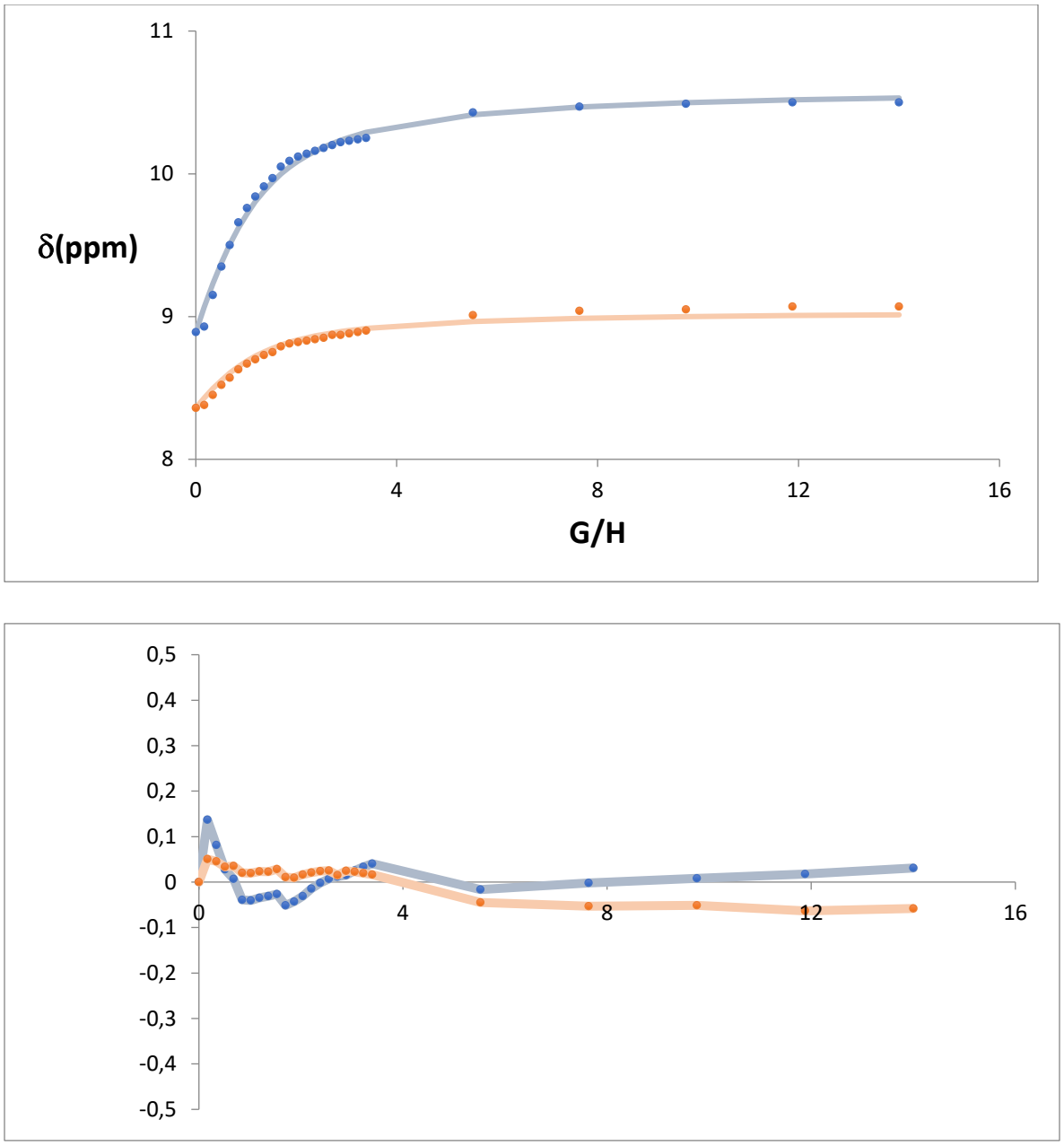

Figure S32. Representation of the δ against $[C_6H_5CO_2^-]/[H_3(\mathbf{2})](OTf)_3]$. Blue and orange dots represent the experimental values, and solid lines represent the output fitting curve according to the H:G model used. The best fitting corresponds to a 1:1 model. This is also in accordance with the distribution of residual errors for the 1:1 model and output errors.

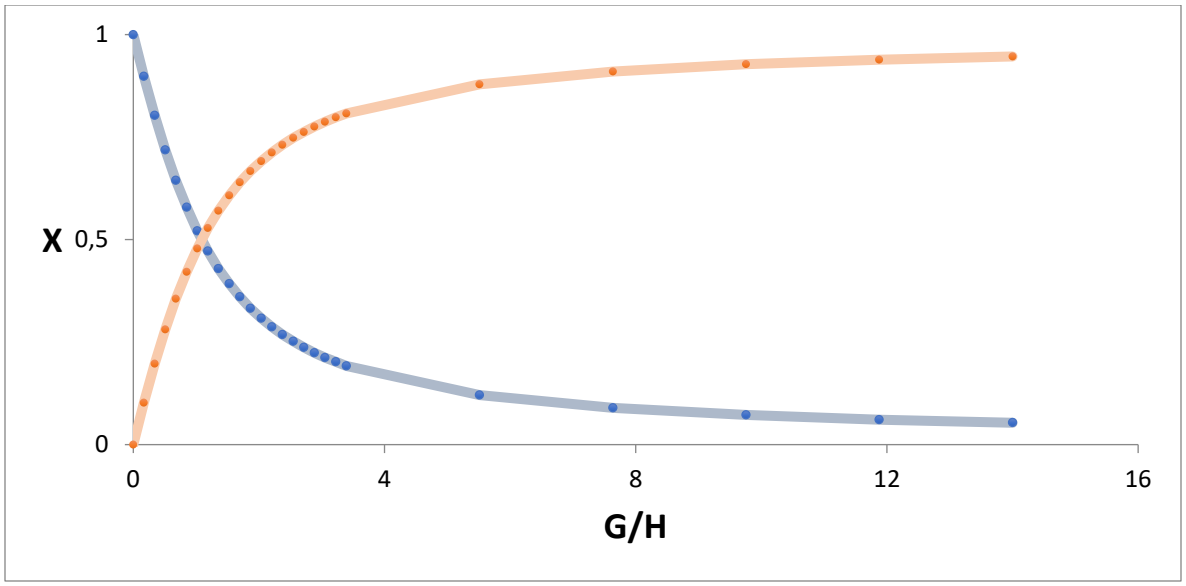

Figure S33. Speciation profile of the titration derived from by the fit of the titration data to a theoretical 1:1 binding model.

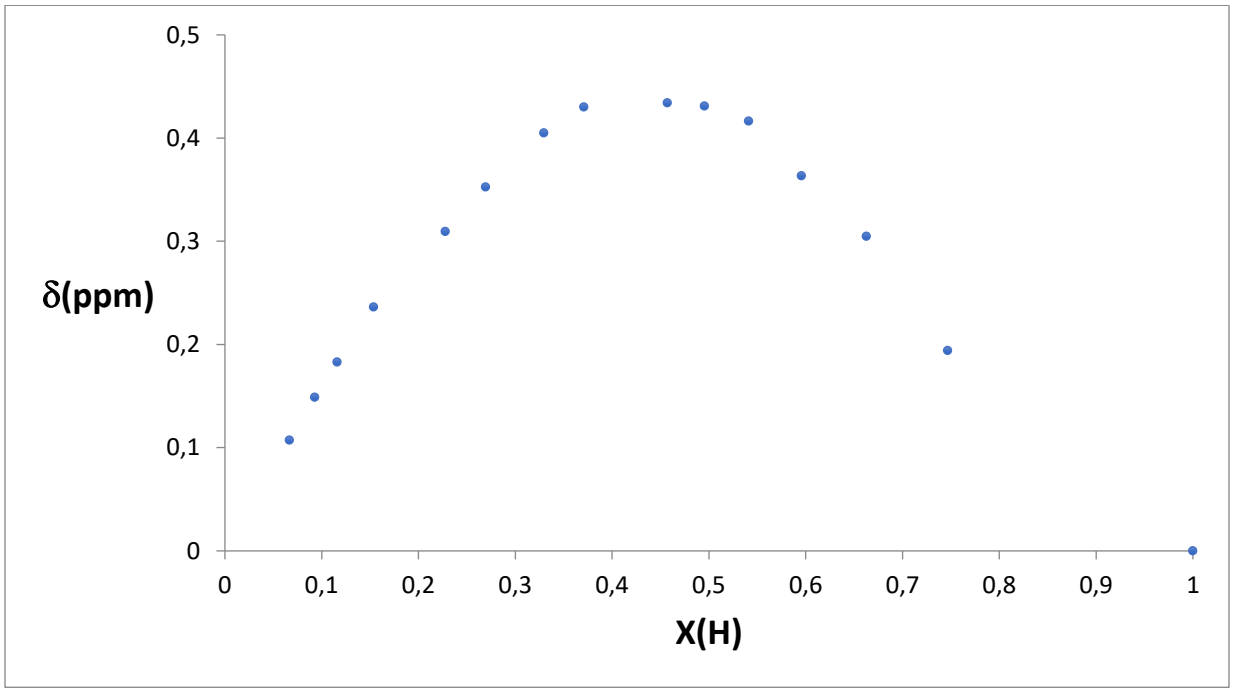

Figure S34: Job plot in CD_3CN for the interaction of $[H_3(\mathbf{2})](OTf)_3$ and $[NBu_4]^+C_6H_5CO_2^-$ showing the 1:1 stoichiometry at 298 K.

Entry	**Anion**	**Host K_{11} [M^{-1}] [a]**
1	Cl	1211 (6%)
2	Br	418 (4%)
3	I	209 (3%)
4	Tosylate	315 (4%)
5	Benzoate	903 (6%)

[a] Errors are given in parentheses.

Table S6. Binding constants of $[H_3(\mathbf{2})](OTf)_3$ with $[NBu_4]^+X^-$ with X^- = Cl, Br, I, $C_7H_{10}SO_3^-$ and $C_6H_5CO_2^-$, as $[NBu_4]^+$ salts in CD_3CN at 25 ^oC.

S4. X-Ray Diffraction studies:

Single crystals of $[H_3(\mathbf{2})](OTf)_3$ $[Ag_3(\mathbf{2})_2](Cl)_3$ and $[Au_3(\mathbf{2})_2](Cl)_3$ suitable for X-ray crystallographic analysis were obtained by slow vapour diffusion of diethyl ether into a dichloromethane solution of $[H_3(\mathbf{2})](OTf)_3$ $[Ag_3(\mathbf{2})_2](Cl)_3$ and $[Au_3(\mathbf{2})_2](Cl)_3$ respectively. Diffraction data were collected on a Agilent SuperNova diffractometer equipped with an Altas CCD detector using Cu Kα radiation (λ = 1.54184 Å). Single crystal was mounted on a MicroMount polymer tip (MiteGen) in a random orientation. The crystals were kept during data collection at 150 K for $[H_3(\mathbf{2})](OTf)_3$ and 100K for $[Ag_3(\mathbf{2})_2](Cl)_2(AgCl_2)$ and $[Au_3(\mathbf{2})_2](Cl)_3$. The structures were solved by direct methods in SHELXS-97[3] and refined by the full-matrix method based on F^2 with the program SHELXL-97 using the OLEX software package.[3-4] Key details of the crystal and structure refinement data for compounds $[H_3(\mathbf{2})](OTf)_3$, $[Ag_3(\mathbf{2})_2](Cl)_2(AgCl_2)$ and $[Au_3(\mathbf{2})_2](Cl)_3$ are summarized below. Further crystallographic data may be found in the corresponding CIF file which was deposited at the Cambridge Crystallographic Data Centre CCDC, Cambridge, UK. The reference numbers for $[H_3(\mathbf{2})](OTf)_3$, $[Ag_3(\mathbf{2})_2](Cl)_2(AgCl_2)$ and $[Au_3(\mathbf{2})_2](Cl)_3$ were assigned as CCDC 1881940, 1881941 and 1881942.

Data refinement for $[Ag_3(\mathbf{2})_2](Cl)_2(AgCl_2)$, proved difficult due to an important disorder of solvent molecules and the counterions chloride and $AgCl_2^-$, which could not be resolved. In addition Ag4 atom was found located at the inversion center (occupancy 1, xtal 0.5). Refinement (R= 0.1083) was obtained when SQUEEZE methodology was applied. CheckCIF/PLATON report shows three alerts of type A: PLAT260 (Large Average Ueq of Residue Including Ag4 0.240, Cl1A 0.256, and Cl5 0.489). Response to all three alerts: A large average Ueq value for a residue may indicate refinement with a too high (possibly fixed) population parameter value. According to their large atomic displacement parameters (Ueq), a one Cl^- and a $AgCl_2^-$ counterion are disordered over two different positions at least, which should account for an atom occupancy of 1. However, we were not able to model only one position with a partial occupancy. The structure model contains large voids with disordered and weak electronic density, which made impossible to model the other positions of the Cl^- and $AgCl_2^-$ anions. In the case of $[Au_3(\mathbf{2})_2](Cl)_3$, high light sensibility and low thermal stability of the crystals was observed. Despite several data sets were collected with different crystals, in all cases the same molecular structure was found. Data refinement proved difficult due to a poor diffraction along with an important disorder due to 1,2-dichloroethane, which could not be satisfactorily resolved.

Refinement (R= 0.1121) was only obtained when SQUEEZE methodology was applied after all solvent molecules were removed from the asymmetric unit. Unfortunately, despite all our attempts a satisfactory refinement could not be accomplished.

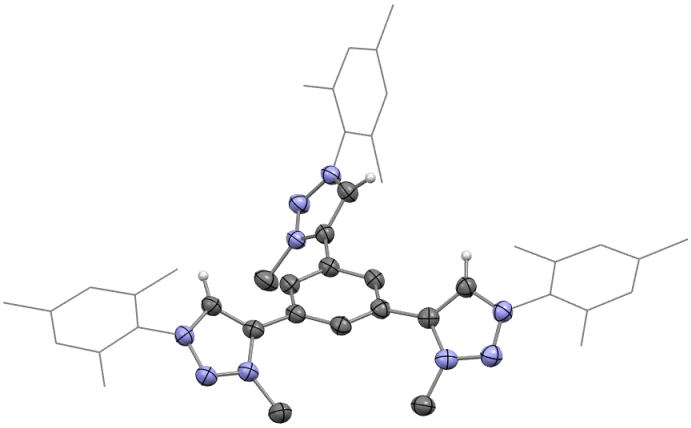

Figure S35: Molecular structure of $[H_3(\mathbf{2})](OTf)_3$. Hydrogen atoms (except triazolium C-H) and counterions (OTf) have been omitted for clarity. Ellipsoids at 50% of probability.

Crystal Data for $[H_3(\mathbf{2})](OTf)_3$: $C_{51}H_{51}F_9N_3O_{10}S_3$ (M =1133.12 g/mol): monoclinic, space group $P2_1/c$ (no. 14), a = 19.1321(3) Å, b = 16.78940(18) Å, c = 17.9660(3) Å, β = 114.4845(17)°, V = 5252.02(14) Å^3, Z = 4, T = 200.00(10) K, μ(CuKα) = 2.100 mm^{-1}, *Dcalc* = 1.433 g/cm^3, 47230 reflections measured (7.314° ≤ 2Θ ≤ 133.168°), 9277 unique (R_{int} = 0.0472, R_{sigma} = 0.0236) which were used in all calculations. The final R_1 was 0.0587 (I > 2σ(I)) and wR_2 was 0.1747 (all data).

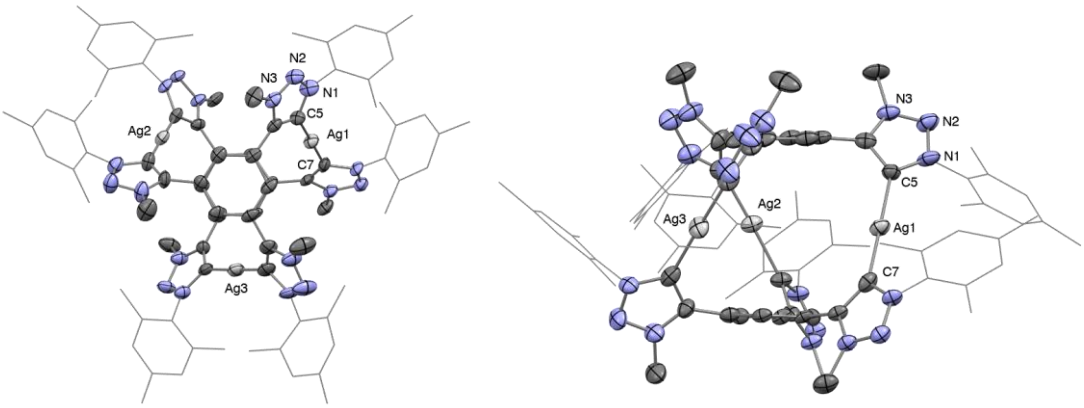

Figure S36: Two perspectives for the molecular structure for $[Ag_3(\mathbf{2})_2](Cl)_2(AgCl_2)$, top (left), side view (right) Hydrogen atoms and counterions (2 Cl^- and 1 $AgCl_2^-$) have been omitted for clarity. Ellipsoids at

50% of probability. Selected bond distances (Å) and bond angles (º): Ag1-C5 2.080(10), Ag1-C7 2.057(12); C7-Ag1-C5 176.9(5), C4-C5-N1 100.4(9).

Crystal Data for $[Ag_3(\mathbf{2})_2](Cl)_2(AgCl_2)$: $C_{168}H_{180}Ag_7Cl_6N_{36}$ (M =3671.26 g/mol): triclinic, space group P-1 (no. 2), a = 16.6514(13) Å, b = 17.4221(12) Å, c = 22.2686(17) Å, α = 79.415(4)°, β = 69.950(4)°, γ = 62.268(3)°, V = 5369.3(7) Å^3, Z = 1, T = 100.0 K, μ(MoKα) = 0.748 mm^{-1}, $Dcalc$ = 1.135 g/cm^3, 108543 reflections measured (4.074° ≤ 2Θ ≤ 53.46°), 22017 unique (R_{int} = 0.1904, R_{sigma} = 0.1965) which were used in all calculations. The final R_1 was 0.1083 (I > 2σ(I)) and wR_2 was 0.3322 (all data).

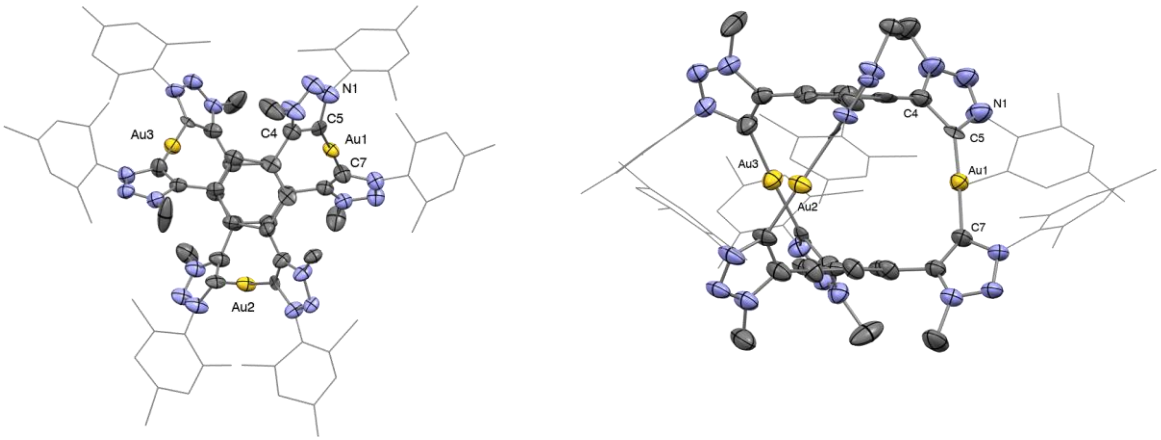

Figure S37: Two perspectives for the molecular structure for $[Au_3(\mathbf{2})_2](Cl)_3$, top (left), side view (right) Hydrogen atoms and counterions $(Cl^-)_3$ have been omitted for clarity. Ellipsoids at 50% of probability. Selected bond distances (Å) and bond angles (º): Au1-C5 1.95(3), Ag1-C7 1.96(3); C7-Ag1-C5 177.7(14), C4-C5-N1 99.0(3).

Crystal Data for $[Au_3(\mathbf{2})_2](Cl)_3$ $C_{86}H_{92}Au_3Cl_7N_{18}$ (M =2216.82 g/mol): monoclinic, space group $P2_1/c$ (no. 14), a = 27.322(7) Å, b = 15.215(4) Å, c = 33.220(9) Å, β = 93.351(6)°, V = 13786(6) Å^3, Z = 4, T = 100.0 K, μ(MoKα) = 3.355 mm^{-1}, $Dcalc$ = 1.068 g/cm^3, 133750 reflections measured (3.982° ≤ 2Θ ≤ 55.25°), 31149 unique (R_{int} = 0.2624, R_{sigma} = 0.5114) which were used in all calculations. The final R_1 was 0.1121 (I > 2σ(I)) and wR_2 was 0.3195 (all data).

S5. References:

(1) Lim, S. H.; Su, Y.; Cohen, S. M. Supramolecular Tetrahedra of Phosphines and Coinage Metals. *Angew. Chemie* **2012**, *124* (21), 5196–5199.

(2) Ugi, I.; Perlinger, H.; Behringer, L. *Chem. Ber.* **1958**, *91*, 2330–2336. *Caution:* While we have not encountered difficulties in working with MesN3, aryl azides, in particular 2,6-disubstituted substrates, are potentially hazardous and can decompose explosively. These reactions should not be scaled-up without carefully evaluating their safety. In particular, these substrates should *NOT* be purified by distillation. We find that crude MesN3 is easily purified by passage on a silica plug using pentane as eluent and evaporation of the solvents under reduced pressure *at room temperature.*

(3) Bidal, Y. D.; Lesieur, M.; Melaimi, M.; Nahra, F.; Cordes, D. B.; Athukorala Arachchige, K. S.; Slawin, A. M. Z.; Bertrand, G.; Cazin, C. S. J. Copper(I) Complexes Bearing Carbenes Beyond Classical N-Heterocyclic Carbenes: Synthesis and Catalytic Activity in "Click Chemistry." *Adv. Synth. Catal.* **2015**, *357* (14-15), 3155–3161.

(4) O. V. Dolomanov, L. J. Bourhis, R. J. Gildea, J. A. K. Howard and H. Puschmann, *J. Appl. Crystallogr.*, 2009, **42**, 339-341.

(5) G. M. Sheldrick, *Acta Crystallogr. A*, 2008, **64**, 112-122.